ELSEVIER

Journal of Structural Geology 28 (2006) 474–493

JOURNAL OF STRUCTURAL GEOLOGY

www.elsevier.com/locate/jsg

Three-dimensional kinematic history at an oblique ramp, Leamington zone, Sevier belt, Utah

Sanghoon Kwon [a,*], Gautam Mitra [b]

[a] *Department of Earth System Sciences, Yonsei University, Seoul 120-749, South Korea*
[b] *Department of Earth and Environmental Sciences, University of Rochester, Rochester, NY 14627, USA*

Received 25 March 2004; received in revised form 2 June 2005; accepted 22 December 2005

Abstract

Differences in kinematics in adjoining salients in fold–thrust belts are typically accommodated along bounding transverse zones. The Leamington zone is an oblique ramp that accommodates slip between structures in the Provo salient and the central Utah segment of the Sevier fold–thrust belt. The Leamington zone consists of the Leamington Canyon thrust, associated second-order asymmetric folds and an out-of-syncline reverse fault. The Leamington Canyon thrust is a rotated, SE-dipping thrust fault with top-to-southeast motion; it represents an oblique ramp of the folded Canyon Range thrust. Fold tightening of the syncline SE of the folded Leamington Canyon thrust trace during later emplacement of underlying structures, caused out-of-syncline reverse faulting in the fold-core.

Analysis of the finite strain, minor fault populations, and conjugate fracture sets were used in interpreting the 3-D kinematic history along the Leamington zone. Restored maximum stretching directions of finite strain ellipsoids trend eastward overall. Inferred motion planes from populations of slickenlines on minor faults are consistent with overall southeastward motion. Acute bisectors of conjugate fracture sets may reflect more southward directions later in the deformation history. These superimposed deformations, with local relative chronologies of plastic and brittle structures using cross-cutting relationships, indicate that the Leamington zone area shows overall clockwise changes in kinematic directions from E to ESE to SSE during successive pulses of deformation.

The temporal changes in kinematic directions along the Leamington zone most likely reflect variations in kinematics over the oblique ramp as the overall easterly displaced 3-D fold–thrust belt wedge interacted with the pre-existing oblique ramp structure, with small magnitudes of superimposed local vertical-axis rotations during later folding and fold-tightening of the Leamington Canyon thrust.

Keywords: Kinematic history; Oblique ramp; Leamington zone; 3-D strain ellipsoid; Maximum stretching direction; Maximum shortening direction

1. Introduction

Most fold–thrust belts have prominent arcuate map patterns (e.g. Himalayas and Alps), with thrust traces strongly convex toward the foreland. This pattern of convexity is observed at different scales, giving rise to a pattern of salients. Adjoining salients generally exhibit significant variations in their structural styles and deformation histories, such as differences in internal geometries, frequency of imbrication, and variations in displacement field (Mitra, 1997). These differences in kinematics are accommodated along transverse zones, which correspond to recesses, with the traces of major faults trending at high angle to the regional trends (e.g. Thomas, 1990). Transverse zones can originate in a variety of ways. Some may form by mechanisms operating during thrusting, and others by mechanisms that operate subsequent to thrusting (e.g. Kulik and Schmidt, 1988; Thomas, 1990; Paulsen and Marshak, 1997); for example, they may form as transport parallel tear faults or lateral ramps or as transport oblique transfer faults or oblique ramps. However, many are long-lived weak zones that preceded thrusting and controlled lateral variations in basin geometry across which there are dramatic differences in stratigraphy (Thomas, 1990; Mitra, 1997; Paulsen and Marshak, 1999). On either side of a zone, shortening is accommodated on different sets of thrusts in adjoining salients although the total amount of shortening at the décollement level is approximately equal (Mitra, 1997). Thus transverse zones may preserve complex 3-D deformational characteristics.

For tear faults, differences in structural styles across the zone result in abrupt discontinuities while lateral ramps often show truncated structures resulting from strike-slip motion.

* Corresponding author. Tel.: +82 10 9907 3565.
E-mail address: skwon@yonsei.ac.kr (S. Kwon).

0191-8141/$ - see front matter © 2006 Elsevier Ltd. All rights reserved.
doi:10.1016/j.jsg.2005.12.011

Oblique ramps, on the other hand, have more gradual and continuous transitions between structural patterns on either side of the ramp. Therefore, more continuous deformation patterns are likely preserved along oblique ramps.

The Leamington zone in central Utah provides an excellent example of an oblique ramp that records the deformation history during interaction of the Provo salient with the adjoining central Utah segment of the Sevier fold–thrust belt. We studied the structural geometry and kinematics of the Leamington zone in order to constrain the 3-D deformation history of an oblique ramp. We also undertook 3-D strain, fault motion and fracture population studies for the possible sources of observed changes in kinematic directions at the oblique ramp.

2. Geological setting

The Leamington zone lies along the boundary between the Provo salient and the central Utah segment of the Sevier fold–thrust belt (Fig. 1). Distinct differences in stratigraphy and large-scale structural geometry occur across the zone. The zone trends WSW–ENE over 50 km from Leamington to Nephi in west-central Utah, and forms a distinctive physiographic feature that cuts obliquely across the trend of the Sevier fold–thrust belt (Fig. 1).

2.1. Tectonic framework

The Sevier fold–thrust belt is an east-verging zone that defines the eastern margin of thin-skinned crustal shortening in the Cordilleran orogen of western North America (Armstrong, 1968; Burchfiel and Davis, 1975; Allmendinger, 1992; Miller et al., 1992). Within this belt, thrusting displaced Proterozoic, Paleozoic, and Mesozoic miogeoclinal rocks eastward during the late Cretaceous–Paleocene (~140–55 Ma) Sevier orogeny (Armstrong, 1968; Burchfiel and Davis, 1975; Schwartz and DeCelles, 1988). Thrusting decreased overall in age from west to east (Armstrong, 1968), although some older thrust faults were reactivated during the later phases of the orogeny (DeCelles et al., 1995; Mitra, 1997). Following crustal shortening, the belt experienced middle Eocene–early Miocene (~49–20 Ma) local extension of the thrust wedge and Miocene to recent Basin-and-Range regional crustal extension (Constenius, 1996, 1998).

The Sevier fold–thrust belt is broken up into a series of *salients* (where thrust traces show pronounced convexity toward the foreland) (Marshak, 1988; Thomas, 1990) and *linear segments* (where thrust traces are not curved) (Smith and Bruhn, 1984; Lawton et al., 1994; Lageson and Schmitt, 1995; Mitra, 1997). These salients and linear segments are decoupled from one another along regional transverse zones (Mitra, 1997), some of which form prominent recesses with thrust traces concave toward the foreland. Shortening within individual salients is accommodated on different sets of thrusts (Lawton et al., 1994; Mitra, 1997).

The Provo salient (Fig. 1a) of the Sevier fold–thrust belt displays arcuate thrust traces (Kwon and Mitra, 2004). It is bounded on the north by the Uinta–Cortez axis (also called the Charleston transverse zone; Paulsen and Marshak, 1997) that gives rise to a prominent recess (Fig. 1a). Its southern boundary is the Leamington oblique transverse zone (Lawton et al., 1997), which does not have a distinct recess associated with it. Major west-dipping thrust faults in the salient include, from west to east, the Sheeprock thrust, Tintic Valley thrust, East Tintic–Stockton thrust system, Midas thrust, Charleston–Nebo thrust system, and frontal blind thrusts that form a triangle zone adjacent to the undeformed foreland (Fig. 1) (Morris and Shepard, 1964; Black, 1965; Mabey and Morris, 1967; Morris and Lovering, 1979; Christie-Blick, 1983; Morris, 1983; Tooker, 1983; Smith and Bruhn, 1984; Lawton, 1985; Bruhn et al., 1986; Mitra, 1997; Mukul and Mitra, 1998a). Most internal thrust sheets initially developed by fault propagation folding, and then experienced fault-bend folding as they were carried over large ramps (Mitra, 1997). Individual internal thrust sheets (e.g. Sheeprock sheet) show evidence of early penetrative layer-parallel shortening followed by fault-parallel shear. The Sheeprock hanging wall shows layer-parallel shortening strains of 9–18% (average 13.5%), while the footwall (trailing edge of the Tintic Valley sheet) has 5–12% (average 8.5%) layer-parallel shortening (Mukul and Mitra, 1998b). External sheets (e.g. the Nebo sheet and its footwall) show early layer-parallel shortening in the form of spaced (pressure solution) cleavage and weakly deformed fossils in Mesozoic carbonate rocks (Mukul and Mitra, 1998b), but strains are not very large (typically less than 10%) (Mitra, 1997). Strain intensities between thrust sheets, however, have to be carefully compared, particularly for low strain areas where uncertainties can be caused from primary sedimentary fabrics and lithologic controls.

South of the Leamington zone, the central Utah (Pavant) segment of the Sevier fold–thrust belt is the area where the Sevier fold–thrust belt was originally defined by Armstrong (1968). Major thrusts in this segment include, from west to east, the Canyon Range, Pavant, Paxton and Gunnison thrusts and blind triangle zones associated with the last two thrusts (Fig. 1) (Christiansen, 1952; Armstrong, 1968; Burchfiel and Hickcox, 1972; Higgins, 1982; Lawton, 1982, 1985; Standlee, 1982; Allmendinger et al., 1983; Holladay, 1983; Millard, 1983; Villien and Kligfield, 1986; DeCelles et al., 1993, 1995; Royse, 1993; Pequera et al., 1994; Mitra et al., 1994, 1995; Coogan et al., 1995; Mitra, 1997; Lawton et al., 1997). These thrusts developed sequentially from west to east, but older thrusts were reactivated through parts of the thrusting history (DeCelles et al., 1995). Individual internal thrust sheets (e.g. Canyon Range and Pavant sheets) show evidence of early layer-parallel shortening, but the amount of penetrative layer-parallel shortening (typically 10% or less) is smaller than internal thrust sheets (e.g. Sheeprock sheet) of the Provo salient. The translation along the Canyon Range and Pavant thrusts is significantly larger than that along thrusts in the Provo salient, resulting in similar overall shortening in the two areas.

After initial layer-parallel shortening, the thrust sheets experienced large-scale fault-bend folding during their

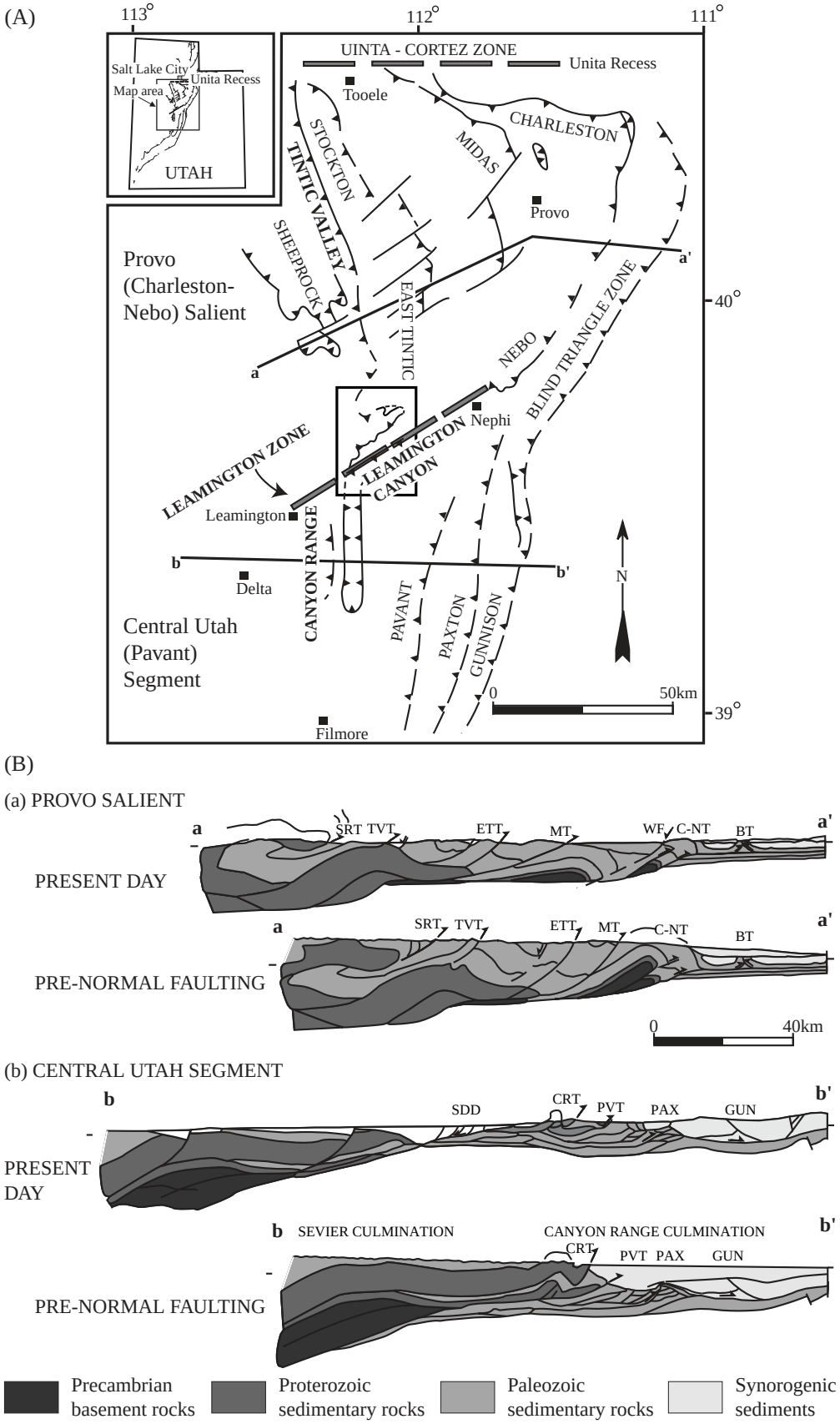

Fig. 1. (a) Map of Provo salient and central Utah segment of the Sevier fold–thrust belt showing the major thrust faults. Lines of cross-sections (AA′ and BB′) are shown. (b) Regional cross-sections: (A) Provo salient and (B) Central Utah segment of the Sevier fold–thrust belt showing present-day (post-normal faulting) configurations, and configurations obtained by restoring the normal faults. Thrusts shown are Sheeprock (SRT), Tintic Valley (TVT), East Tintic (ETT), Midas

emplacement (Fig. 1b). The external thrusts were blind having been covered by syn-orogenic sediments during their emplacement; their structure is known mainly from subsurface (seismic and drill-hole) information (Standlee, 1982; Coogan et al., 1995). Where hanging wall rocks are exposed, the early layer-parallel shortening is preserved in the form of a spaced pressure solution cleavage in carbonate lithologies (Mitra, 1997).

The ENE–WSW Leamington zone is located along the boundary between the Provo salient and the central Utah segment (Fig. 1). The Leamington zone consists of the Leamington Canyon thrust, associated secondary asymmetric folds and an out-of-syncline reverse fault (which are described in detail in a later section). South of the Leamington zone, in the central Utah segment, the Oquirrh section is absent (Hintze, 1988) and isopach maps of Paleozoic strata show that the zone coincides with the southern end of the upper Paleozoic Oquirrh basin (Peterson, 1977; Levy and Christie-Blick, 1989; Royse, 1993; Lawton et al., 1994; Paulsen and Marshak, 1999).

3. Macroscopic and Mesoscopic structures

3.1. Geology of the southern Gilson Mountains/northern Canyon Mountains

The main structures exposed at the transition between the Gilson Mountains and the Canyon Mountains (Fig. 2) are (1) the Tintic Valley thrust (north of the Leamington transverse zone, in the Provo salient); (2) the Canyon Range thrust (south of the Leamington transverse zone, in the central Utah segment); and (3) the Leamington transverse zone that developed along the southern boundary of the Gilson Mountains (Costain, 1960; Wang, 1970; Higgins, 1982; Pampeyan, 1989). At its eastern end (in the Nebo area) (Fig. 1), the Leamington zone has been interpreted as a lateral ramp of the Charleston–Nebo thrust system (Allmendinger, 1992; Constenius, 1998). At its western end, in the Gilson Mountains, the Leamington zone separates two prominent thrusts (namely Tintic Valley thrust and Canyon Range thrust) (Figs. 1 and 2).

The Tintic Valley thrust is well exposed in the eastern half of the Gilson Mountains and its position in the northern portion of the Gilson Mountains has been interpreted in several different ways (Costain, 1960; Wang, 1970; Higgins, 1982; Pampeyan, 1989). Costain (1960) first mapped two high-angle reverse faults in the Gilson Mountains and these faults were later interpreted as the southern end of the folded Tintic Valley thrust (Wang, 1970; Higgins, 1982; Pampeyan, 1989). Morris and Kopf (1969) and Wang (1970) have suggested that the Tintic Valley thrust ends at the eastern end of the southern Gilson Mountains, while others (Higgins, 1982; Pampeyan, 1989) have shown that the Tintic Valley thrust has a leading branch-line with the Leamington Canyon fault at the western end of the southern Gilson Mountains (Fig. 2). Recent detailed studies (Kwon and Mitra, 2001, 2004, 2005) show that the Tintic Valley thrust is a folded thrust fault that carries older Paleozoic strata over younger Paleozoic strata and has a branch-line with the Leamington Canyon thrust in the southwestern part of the Gilson Mountains (Fig. 2).

The Canyon Range thrust sheet and associated hanging wall rocks are folded into a large syncline (i.e. Canyon Range syncline) that is exposed in the middle and eastern part of the Canyon Mountains (Figs. 1 and 2) (Christiansen, 1952; Ismat and Mitra, 2000, 2005). The synclinal trace runs N–S along the middle of the range for much of its length, but bends to the northeast at the northern end, near Leamington Canyon (which includes the Leamington Canyon thrust) (Fig. 2). Even though later Tertiary normal faulting has obscured relationships between the Canyon Range thrust and the Leamington Canyon thrust, Precambrian, Cambrian and Cretaceous hanging wall strata in the west limb of the folded Canyon Range thrust sheet can be traced continuously to the strata in the hanging wall of the Leamington Canyon thrust (Lawton et al., 1997) and have high-angle hanging-wall cutoffs at the thrust in the eastern end of the southern Gilson Mountains (Fig. 2). The continuous stratigraphic section in the hanging wall and the somewhat less continuous section in the footwall suggest that the Leamington Canyon thrust and the Canyon Range thrust are essentially the same fault and there is a large oblique ramp ($\sim$10 km length along the fault) where the fault climbs up-section laterally in its footwall from the lower Paleozoic Sedimentary rocks (i.e. Cambrian Tintic Quartzite) below the Canyon Range thrust to the middle Paleozoic sedimentary rocks (i.e. Mississippian Humbug Formation) below the Leamington Canyon thrust (Sussman, 1995) (Fig. 3).

The observed bending of the synclinal trace from the Canyon Range thrust to the Leamington Canyon thrust can be explained by oblique folding in the hanging wall of the Canyon Range thrust/Leamington Canyon thrust (Pequera et al., 1994). The syncline progressively tightens toward the north, changing from an upright to an overturned fold (refer to fig. 4 of Ismat and Mitra, 2005). In the Canyon Mountains the fold tightening occurred while the Canyon Range thrust sheet was being deformed by a connecting splay duplex (Mitra and Sussman, 1997) that developed in its footwall (Ismat and Mitra, 2000, 2005). The duplex forms the core of the Canyon Range anticline and its growth resulted in the amplification of the anticline and tightening of the adjoining syncline (Mitra and Sussman, 1997). This deformation took place in the elastico-frictional regime by the mechanism of cataclastic flow (Ismat and Mitra, 2000, 2005). In the Gilson Mountains the fold tightening is most likely related to the evolution of the Leamington zone.

The Leamington zone contains the first-order Leamington Canyon thrust, associated second-order and small-scale asymmetric folds, and an out-of-syncline reverse fault (Fig. 2). In the southern Gilson Mountains, the Leamington

(MT), Charleston-Nebo (C-NT), and blind triangle zone (BT) for the Provo Salient, and Canyon Range (CRT), Pavant (PVT), Paxton (PAX) and Gunnison (GUN) for the central Utah segment. Wasatch normal fault (WF, Provo Salient) and Sevier Desert detachment (SDD, central Utah segment) are also shown. Box indicates location of Leamington area shown in more detail in Fig. 2.

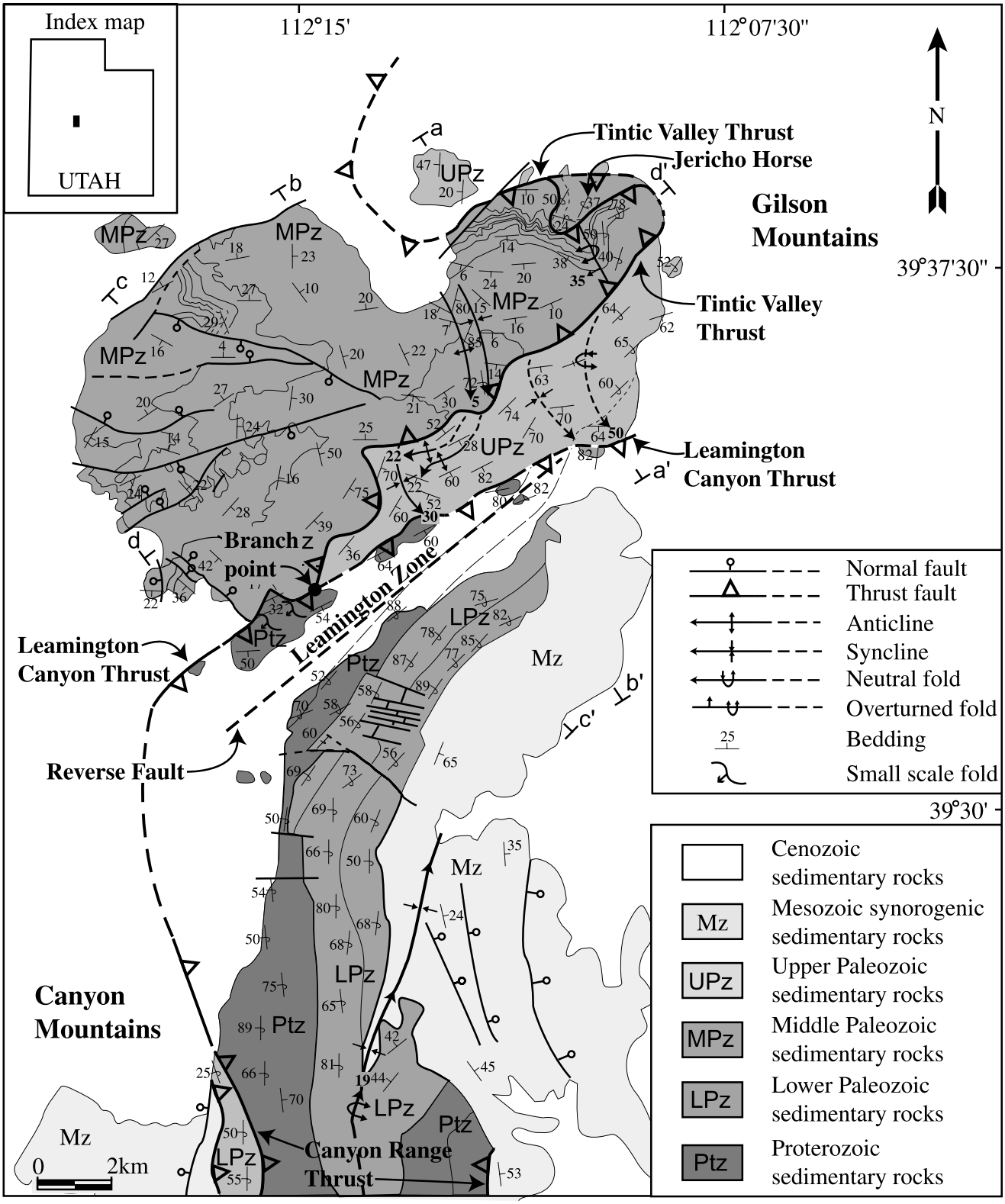

Fig. 2. Detailed geologic map of the Gilson Mountains and northern Canyon Mountains showing the major structures: Leamington zone, Leamington Canyon thrust, Tintic Valley thrust, Jericho horse, Canyon Range thrust and out-of-syncline reverse fault. Inset map shows location of the Gilson Mountains on a map of Utah.

Canyon thrust strikes N60°E, making an angle of 30° to the regional W–E transport direction, and dips steeply toward SE. The fault places Proterozoic and lower Paleozoic quartzites over Paleozoic limestones and sandstones (Fig. 2). In this area, the Leamington Canyon thrust has been variously interpreted as a thrust fault dipping to the southeast with up-dip motion (Costain, 1960; Higgins, 1982), as a tear fault with right-lateral movement (Morris and Shepard, 1964; Wang, 1970; Holladay,

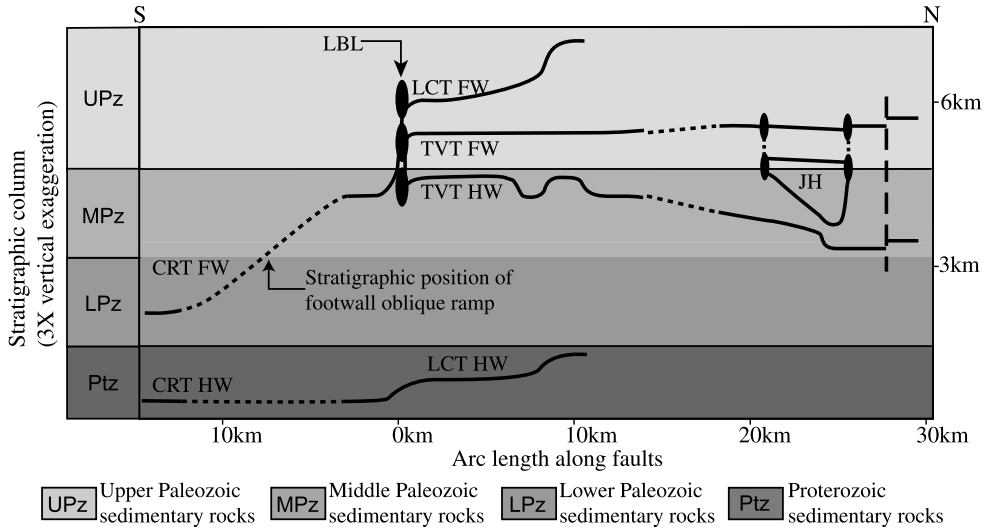

Fig. 3. Strike-parallel stratigraphic-separation diagram of the Canyon Range thrust (CRT), the Leamington Canyon thrust (LCT), the Tintic Valley thrust (TVT), and the Jericho horse (JH). The Tintic Valley thrust joins with the Leamington Canyon thrust along a leading branch line (LBL). The stratigraphic-separation continuously increases as the thrust climbs from lower Paleozoic sedimentary rocks in the footwall (FW) of the Canyon Range thrust to middle Paleozoic sedimentary rocks in the FW of the Leamington Canyon thrust, indicating the existence of a footwall oblique ramp. Maximum stratigraphic-separation is observed along the Leamington Canyon thrust, and the Jericho horse lies in the footwall of the Tintic Valley thrust.

1983) or as a lateral (or oblique) ramp of the Canyon Range thrust (Royse, 1993; Pequera et al., 1994; Sussman, 1995; Lawton et al., 1997; Mitra and Sussman, 1997; Kwon and Mitra, 2001, 2005). These different interpretations raise questions about the nature of motion along the Leamington Canyon thrust and relations to other structures. These questions can be answered by examining the structural geometry and kinematics of motion of the Leamington Canyon thrust.

3.2. Kinematics of motion along the Leamington Canyon thrust

The Leamington Canyon thrust is well exposed in an erosional window in the southwestern Gilson Mountains, with hanging wall rocks showing weak grain shape foliation, asymmetric folds, and fracture populations with slickensides that developed during successive phases of motion on the fault. Bedding in the hanging wall rocks of the Leamington Canyon thrust shows progressive increase in dip from 30 to 80° from west to east along the fault (Fig. 2), indicating that the fault is folded into an antiform along a fold-axis plunging moderately (24°) to the southwest (216°) (Fig. 4a). Although gently dipping fractures are present in the hanging wall and footwall of the Leamington Canyon thrust, the dominant fracture sets are moderate to steeply dipping toward SE (Fig. 4b). The kinematics of movement along fractures in such a population in a single tectonic episode can be demonstrated by plotting the poles to the motion planes (M-planes), or M-poles on a stereographic projection (Arthaud, 1969; Wojtal, 1982; Alexandrowski, 1985; Goldstein and Marshak, 1988; Mitra, 1993). The M-plane for a single fault is defined by the plane

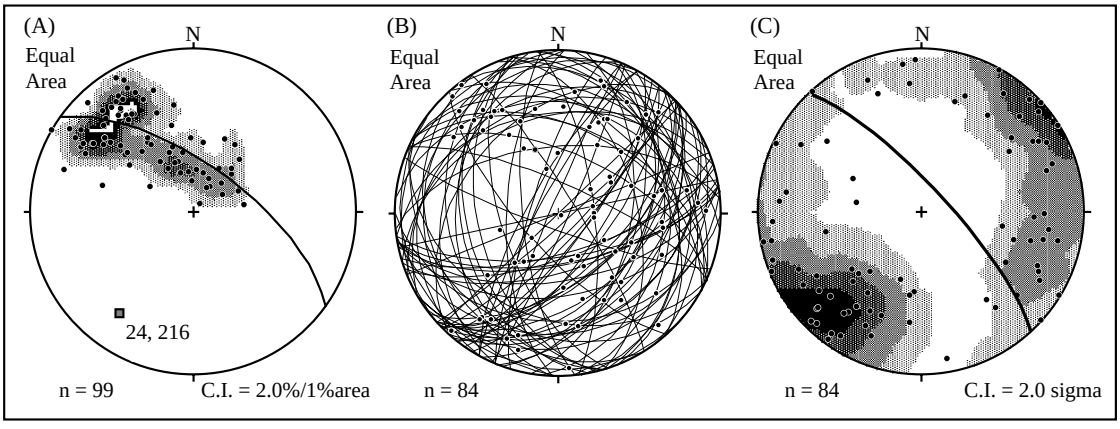

Fig. 4. Contoured equal area stereograms from the hanging wall of the Leamington Canyon thrust for (a) poles to bedding with associated best-fit fold-axis, (b) fractures with slickenlines, and (c) M-poles with associated motion plane (M-plane). M-plane is dipping steeply and trending NW–SE.

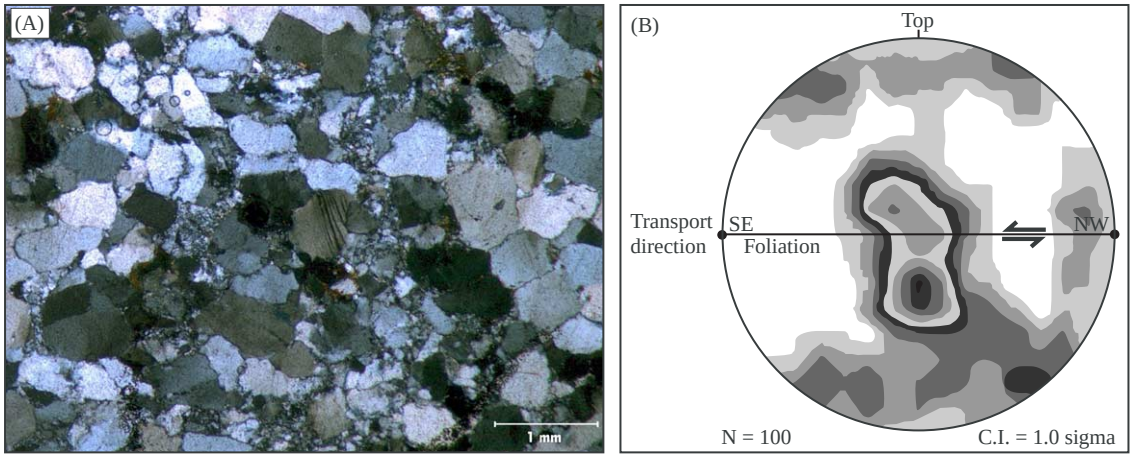

Fig. 5. (a) Photomicrograph of the hanging wall quartzite (Pocatello Formation; sample collected 10 cm from the thrust) of the Leamington Canyon thrust. Cross-polarized light. (b) Lower hemisphere, equal area plot of quartz *c*-axis fabrics viewed towards the SW from the quartzite sample of (a) showing top-to-the-southeast down-dip shear. This is consistent with down-dip motion of the folded Canyon Range thrust sheet farther to the south.

that contains the pole to the fault plane and the slickenside lineation on the fault. For a population of faults, the M-plane is perpendicular to the λ_2 (intermediate shortening) axis and contains λ_1 (maximum shortening) and λ_3 (minimum shortening) axes (Reches, 1978, 1983). The orientations of fractures with slickenlines from the hanging wall of the Leamington Canyon thrust give a consistent M-plane that is steeply dipping and trends NW–SE (Fig. 4c). This indicates that the Leamington Canyon thrust has transported the hanging-wall rocks toward the northwest or the southeast over the footwall strata; the movement direction is almost perpendicular to the trend of the Leamington Canyon thrust. In order to distinguish between the alternative northwest or southeast directions of transport on the M-plane, we measured the lattice preferred orientation of quartz grains from quartzites such as 'Pocatello' of Hintze (1988) and Caddy Canyon Formation in the hanging wall of the Leamington Canyon thrust. The measured pattern of quartz *c*-axes shows asymmetric type I cross girdle (Passchier and Trouw, 1996), indicating top-down to the southeast shear (Fig. 5). This interpretation agrees with the sense of shear determined from acute angles of cleavage-bedding intersections in hanging wall and footwall rocks and from asymmetric folds at various scales.

3.3. Structural geometry of the Leamington Canyon thrust

The structural relationship between the folded Leamington Canyon thrust and the other major structures in the Gilson Mountains are demonstrated in a series of cross-sections (Fig. 6). The key features of the cross-sections, on the basis of orientation data collected in the course of mapping, include the following:

1. The Leamington zone contains the folded Leamington Canyon thrust, associated second-order and smaller asymmetric folds, and an out-of-syncline reverse fault (Fig. 6). The folded Leamington Canyon thrust cuts up stratigraphic section to the southeast placing Proterozoic strata over Paleozoic strata (Fig. 6b and c). The fault is folded into an anticline by the underlying structures (e.g. Tintic Valley thrust and Jericho horse), and the synclinal pair of the antiformally folded Leamington Canyon thrust probably corresponds to the northern end of the Canyon Range syncline (Fig. 6b and c) (Pequera et al., 1994). The second-order asymmetric folds, with hinges parallel to the trend of the Leamington Canyon thrust and moderate plunges, further support our kinematic interpretation (Figs. 4 and 5). Emplacement of the Tintic Valley thrust and the Jericho horse caused tightening of the northern end of the Canyon Range syncline. This tightening probably took place within the elastico-frictional regime by cataclastic flow like in the Canyon Range to the south (Ismat and Mitra, 2000, 2005). Part of the Leamington Canyon thrust was reactivated as an out-of-syncline reverse fault that accommodated slip during fold-tightening (Fig. 6b and c).
2. The Tintic Valley thrust displaced older Paleozoic strata southeastward over younger Paleozoic strata (Figs. 2 and 6b and c). The Tintic Valley thrust is also folded into an anticline/syncline pair by the underlying Jericho horse (Figs. 2 and 6). Our cross-sections and the stratigraphic relationships suggest that the Tintic Valley thrust joins with the Leamington Canyon thrust along a leading branch-line in the southwestern part of the Gilson Mountains (Figs. 2 and 6).
3. The Jericho horse places overturned older Paleozoic strata over younger Paleozoic strata (Figs. 2 and 6). These overturned beds may represent part of a footwall syncline of a fault-propagation fold similar to the pattern suggested by McNaught and Mitra (1993). The reclined folding within the Tintic Valley thrust sheet (Fig. 6) is probably related with refolding of the steep limb of the fault-bend fold associated with Tintic Valley thrust emplacement, during later emplacement of the Jericho horse. The folded SE limb of the synformally folded Tintic Valley thrust (Fig. 6) is probably formed at the same time as this reclined folding. The reclined fold has a fold-axis with a southwesterly trend (212°) and a low plunge (23°) (Fig. 2).

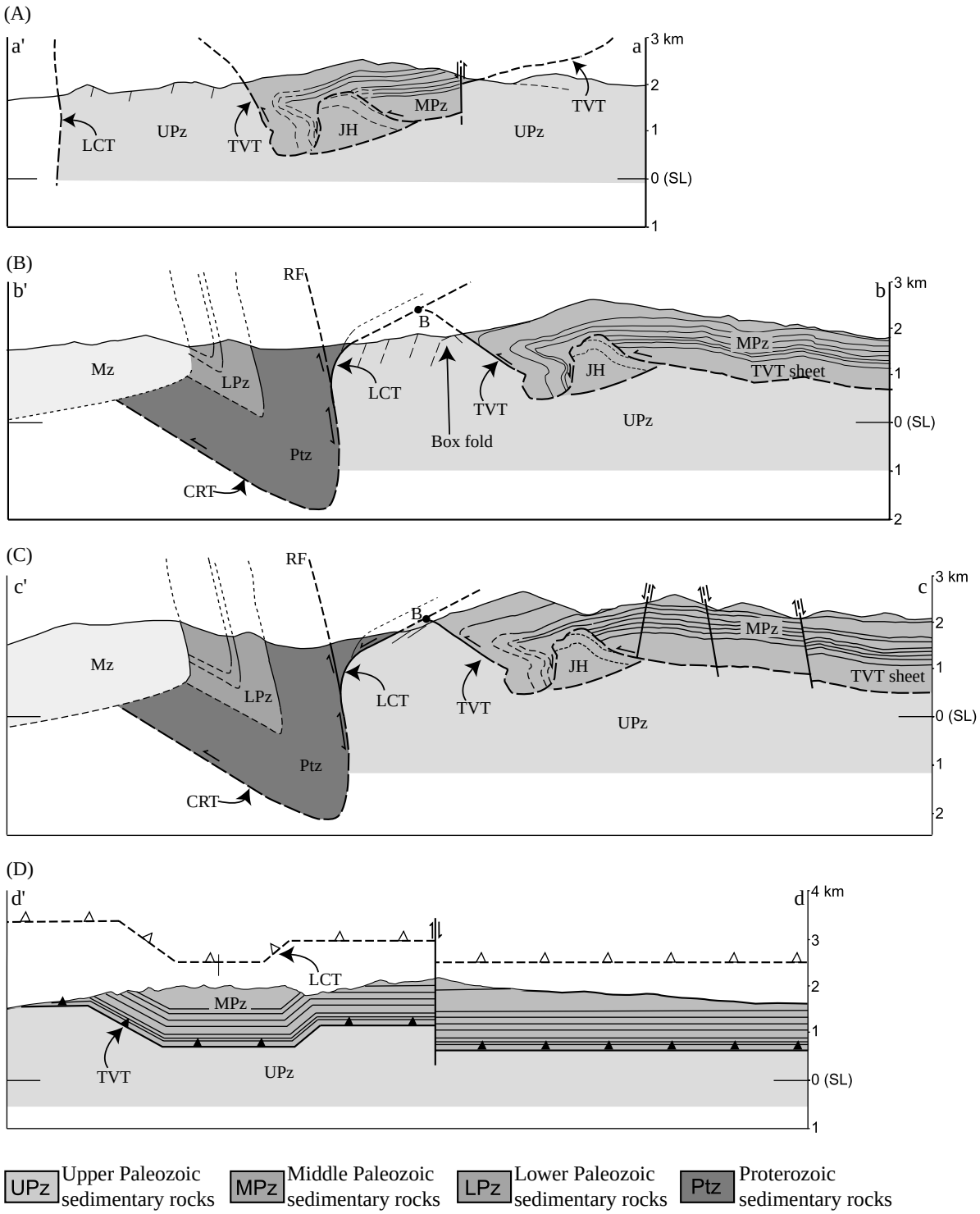

Fig. 6. Cross-sections across the Leamington zone ((A)–(C)) and parallel to the Leamington zone (D), showing major structures and lithologic contacts in the Gilson Mountains. Structures shown are the Canyon Range thrust (CRT), the Leamington Canyon thrust (LCT), the Tintic Valley thrust (TVT), the Jericho horse (JH) and the out-of-syncline reverse fault (RF).

4. The relatively large-scale folds that developed in the common footwall (upper Paleozoic sedimentary rocks) of the Leamington Canyon thrust and the Tintic Valley thrust in the southern Gilson Mountains (Fig. 2) suggest that these rocks experienced a complex deformation history. The central portion of the common footwall contains a box-type fold with two parallel antiformal fold-hinges, and a synformal fold (Fig. 2). The box-type fold (Fig. 6b) has a fold-axis parallel to the trend of the Leamington Canyon thrust (22°, 231°; Fig. 7a), which represents fold-axis orientation before refolding. The synform has a moderately south-plunging fold-axis (30°, 189°; Fig. 7b), which resulted

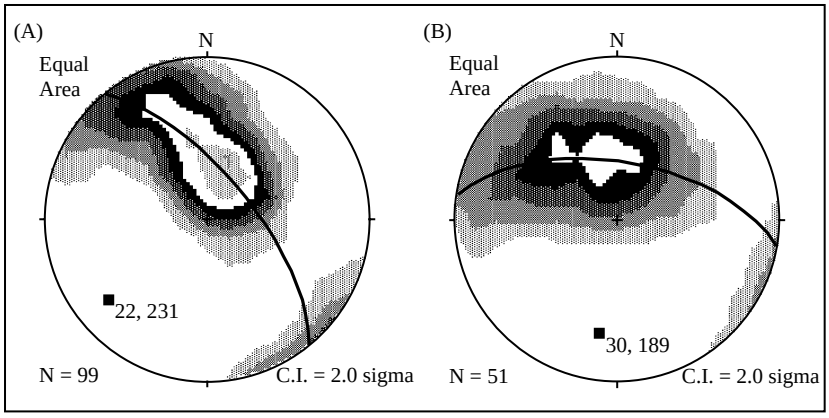

Fig. 7. Contoured equal area plots of bedding from the relatively large-scale folds in the common footwall of the Leamington Canyon thrust and the Tintic Valley thrust. The box-type fold with two antiformal fold-hinges, plunging moderately to the southwest (22°, 231°) (a), represents the fold-axis before refolding; the adjoining synformal fold-hinge, plunging moderately to the south (30°, 189°) (b), represents the fold-axis during refolding.

from a later refolding during the emplacement of underlying structures such as the Jericho horse and blind thrusts. The neutral fold observed in the eastern part of the common footwall (Fig. 2) probably formed as part of the same fold system as the box-type fold. Two alternative interpretations for the relative timing of the folds observed in the common footwall, with respect to the major structures in the study area, will be addressed in the following section on the structural evolution of the Leamington zone.

From all of the evidence, the folded Leamington Canyon thrust is essentially the same fault as the folded Canyon Range thrust to the south, and serves not only as an oblique ramp of the folded Canyon Range thrust, but also as a termination for the Tintic Valley thrust to the north. Therefore, the Leamington zone, including the Leamington Canyon thrust most likely served as a slip accommodation zone between structures at the boundary between two prominent segments of the Sevier fold–thrust belt (namely the Provo salient and the central Utah segment).

3.4. Structural evolution of the Leamington zone

The evolution of structures in the area of the Leamington zone can be demonstrated in the context of regional relations by drawing a series of sequentially retrodeformed cross-sections (Fig. 8). Because the line of cross-section is oblique to the W–E regional transport direction, it is not possible to rigorously balance the cross-section. However, the cross-section is admissible as it illustrates realistic geometries observed in the area.

The Leamington Canyon thrust was the first-formed fault among the observed thrust faults within the Gilson Mountains, and placed a section including Proterozoic to early Paleozoic rocks on top of late Paleozoic strata. In the southern Gilson Mountains, the Leamington Canyon thrust appears as a near bedding-plane parallel fault juxtaposing Proterozoic quartzites with late Paleozoic strata. Farther to the northeast, Proterozoic and early Paleozoic Formations change dips to almost vertical and have hanging wall cutoffs along the Leamington Canyon thrust (Fig. 2), thus placing hanging wall ramp on footwall flat (Fig. 6b and c). This gives a minimum displacement of ~27 km based on local restoration (Fig. 8a). After the initial emplacement of the Leamington Canyon thrust, the Tintic Valley thrust branched out and ramped up through the anticlinal hinge region and developed a relatively large-scale horse (Tintic Valley thrust sheet), leaving a footwall syncline at the base of the thrust ramp (Fig. 8b). The fault merges with the Leamington Canyon thrust at a leading branch line creating a horse that was transported southeastward producing a fault-bend fold (Fig. 8c). At this stage, a lower fault branched from the Tintic Valley thrust, cut through the synclinal hinge region truncating overturned beds of the footwall syncline, and rejoined the Tintic Valley thrust to form a small-scale horse, the Jericho horse (Fig. 8c). The Jericho horse was transported southeastward causing more refolding of pre-existing folds, and resulting in reclined folding in the southeastern part of the Tintic Valley thrust sheet (Figs. 6 and 8d). Minimum displacements of the Tintic Valley thrust sheet and the Jericho horse are ~6 and 5 km, respectively. Fold-tightening of the Leamington Canyon thrust by the underlying Tintic Valley thrust and Jericho horse caused out-of-syncline reverse faulting from the synclinal core of the folded Leamington Canyon thrust; part of the Leamington Canyon thrust was probably reactivated at this time.

The relative timing of folding observed in the common footwall of the Leamington Canyon thrust and the Tintic Valley thrust can be explained by two alternative kinematic interpretations (Fig. 9). The first possibility is that the box-type fold with two antiformal fold-hinges is related to detachment folding (or fault-propagation folding) associated with the Tintic Valley thrust (Fig. 9a). In this case, the box-type folding can be explained as a remnant of the Tintic Valley thrust fault-propagation fold (or detachment fold) that was left in the footwall as a result of high angle breakthrough (Suppe and Medwedeff, 1990). This fold experienced refolding during the emplacement of the Jericho horse (Fig. 9a). Therefore, in the first possibility, the thrusting in the study area experienced an overall break forward sequence.

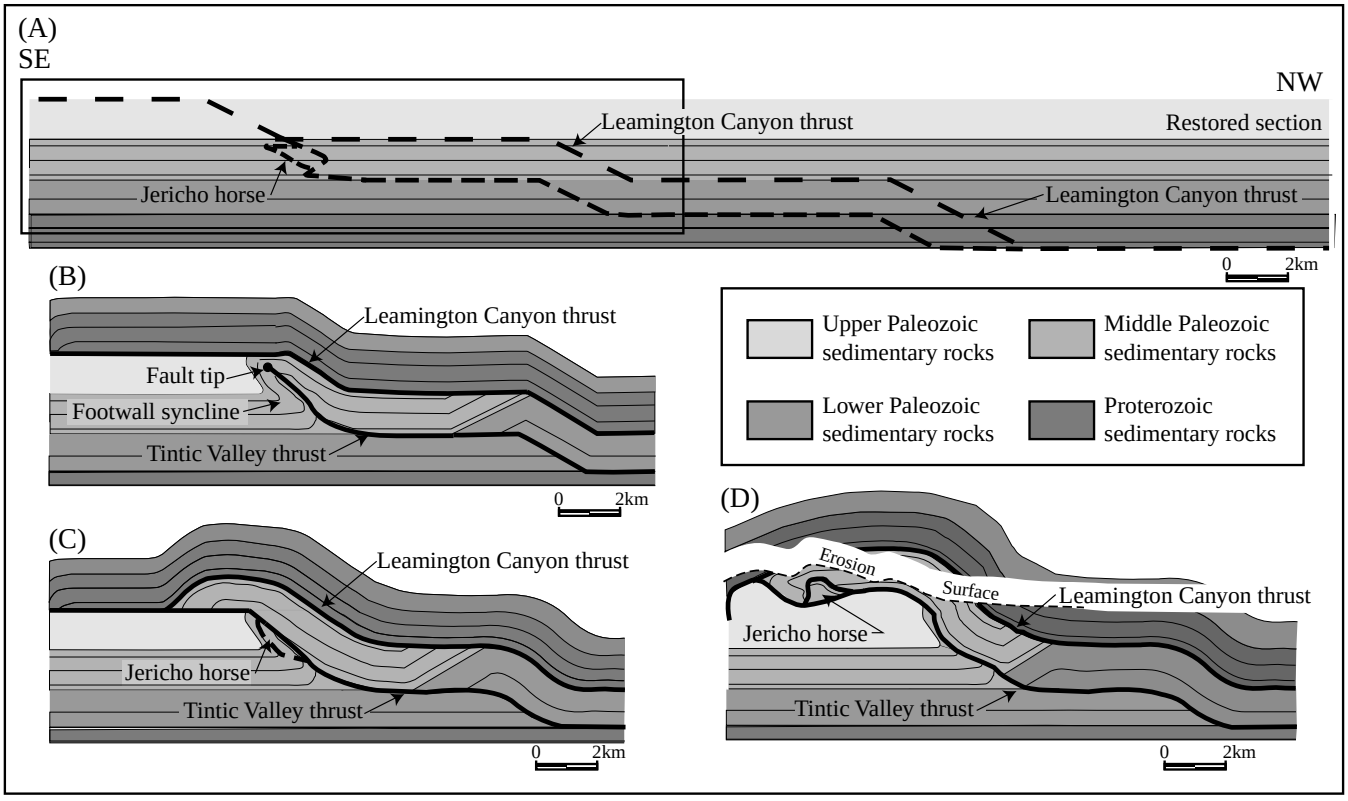

Fig. 8. Sequentially retrodeformed cross-sections based on a down-plunge projection (looking SW) of major structures in the Gilson Mountains. Azimuth of projection plane is similar to cc′ on Fig. 2. Thrusts shown are the Leamington Canyon thrust, the Tintic Valley thrust and the Jericho horse. Rectangular box shown in (a) is enlarged in (b)–(d). The trailing branch line (outside the box) along the contact between lower Paleozoic and Proterozoic rocks moves toward the SE from (a) to (d). (a) Restored section where the restoration has been carried out for most of the major structures. (b) Emplacement of the Leamington Canyon thrust and development of the Tintic Valley thrust sheet with attendant detachment (or fault-propagation) folding. (c) Emplacement of the Tintic Valley thrust sheet with fault-bend folding and the formation of the small-scale Jericho horse from the footwall syncline of the Tintic Valley thrust detachment (or fault-propagation) fold. (d) Emplacement of the Jericho horse causing reclined folding within the Tintic Valley thrust sheet.

Alternatively, the box-type folding can be related with an unexposed blind thrust underlying the Tintic Valley thrust (Fig. 9b); so that the box-type fold can be a detachment fold or a fault-propagation fold, which was formed at the tip of the blind thrust (Fig. 9b). In this case, the earlier box-type fold experienced refolding associated with the formation of the Jericho horse (Fig. 9b) in a break-back sequence.

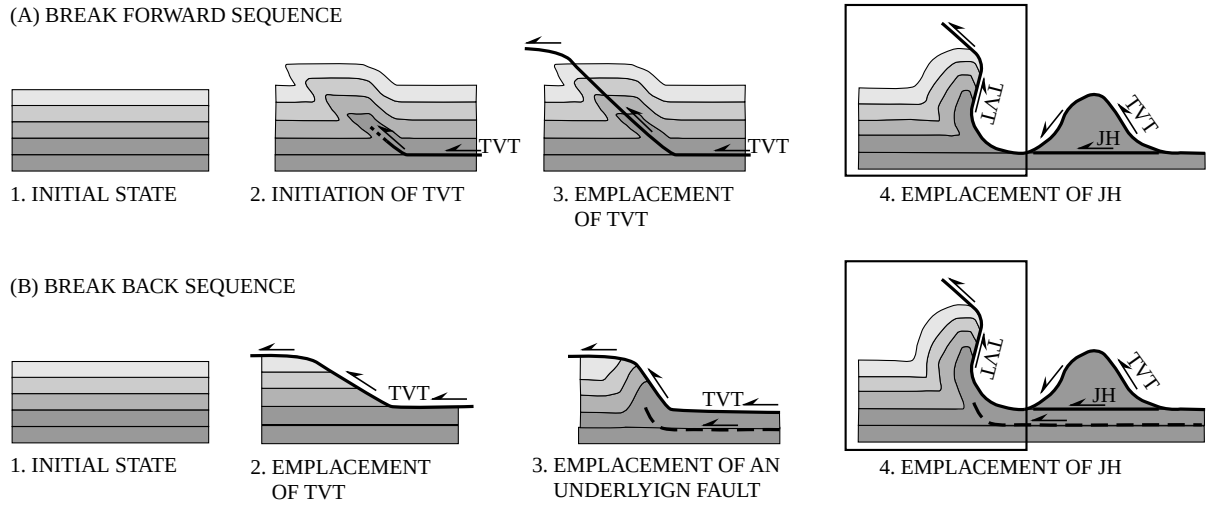

Fig. 9. Alternative conceptual models to explain the kinematic evolution of the footwall deformation with respect to major structures. The figures are schematic and not to scale. The boxed parts of the figures show simplified versions of the structures exposed in the footwall of the Tintic Valley thrust. Thrusts shown are the Tintic Valley thrust (TVT) and the Jericho horse (JH).

The folded SE limb of the synformally folded Tintic Valley thrust and the neutral fold observed in the common footwall were probably formed as a part of the same system as the refolded box-type fold.

4. Microstructures

Detailed studies on microstructures developed within the hanging wall quartzites of the Leamington Canyon thrust have allowed us to work out the emplacement conditions (Sussman, 1995; Mitra and Sussman, 1997). We looked at microstructures from hanging wall quartzites of the Leamington Canyon thrust, where the rocks have a weak foliation defined by grain shape preferred orientation. The host quartz grains show earlier features of diagenesis characterized by very 'clean' reprecipitation with no preferred orientation (Fig. 10a). Cross-cutting relationship between plastic deformation features (e.g. undulose extinction, intragranular cracks, deformation bands and serrated grain boundaries) and cataclastic features (e.g. transgranular cracks and zones of cataclasis) indicate that crystal plastic deformation was followed by cataclasis during progressive deformation.

The earliest phase of deformation is manifested by intragranular micro-cracks (Fig. 10b–d) many of which are preserved as thin healed cracks. These cracks are likely either pre-existing cracks in sedimentary grains or are formed by small plastic strains within grains that lead to stress concentrations at dislocation pile-ups (Mitra, 1978; Ashby et al., 1979). The presence of undulose extinction and poorly developed deformation bands (Fig. 10b and c) indicate that dislocation glide played a role during this early deformation. Possible serrated grain boundaries (Fig. 10d) indicate that dislocation creep (glide and climb) was also involved in deformation. Possible stylolites (Fig. 10b and c) along some grain boundaries indicate deformation by diffusive mass transfer as well. These microstructures suggest that multiple deformation mechanisms were active during deformation.

Later stages of deformation are characterized by variously oriented transgranular cracks and zones of cataclasis that cross-cut the early plastic deformation features (Fig. 10d). The transgranular cracks cut across grain boundaries and show little displacement. Some of these cracks show anastomosing and/or parallel patterns giving rise to lenticular shaped clasts (aggregates of host grains). The cataclasite zones are filled with fragments of host rock and matrix. The development of transgranular and anastomosing cracks, almost parallel to cataclastic zone boundaries, indicate that these zones grew in thickness by fracturing in adjoining rocks to reduce asperities at the wall rock–cataclastic zone boundary (Mitra, 1984). Transgranular cracks that branch from cataclastic zones are observable in thin sections (Fig. 10d). Later phase cracks crosscut the previous features as well as matrix in wider cataclasite zones.

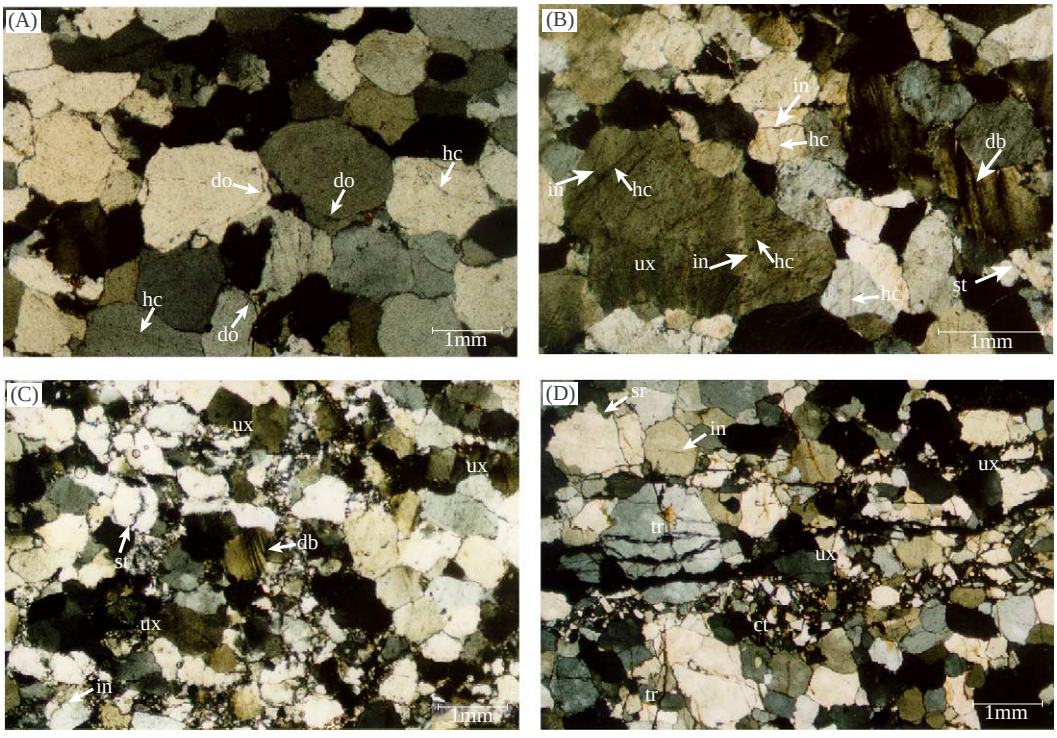

Fig. 10. Photomicrographs of deformed quartzites from the hanging wall of the Leamington Canyon thrust: do—diagenetic overgrowth, hc—healed cracks/fractures, in—intragranular crack, db—deformation band, sr—serrated grain boundary, st—stylolites, ux—undulose extinction, tr—transgranular crack, ct—cataclasite. (a) Diagenetic overgrowths surround the original grain boundaries. Deformation before the formation of the Leamington Canyon thrust is characterized by hc. (b) and (c) Crystal plastic deformation features such as in db, sr, st, and ux; note that intragranular cracks cut across healed cracks. (d) Cataclastic deformation features such as ct and tr, which cut across plastic deformation features.

Table 1
3-D stain data

Sample	A		B		C		Principal strain ratios		k	S_1/S_3	Bedding	Orientations		
	R_f	ϕ	R_f	ϕ	R_f	ϕ	S_1/S_2	S_2/S_3				E_1	E_2	E_3
LC1	1.13	83	1.13	44	1.12	30	1.12	0.93	1.56	1.20	53/142	17/293	71/084	09/200
LC2	1.16	163	1.19	28	1.17	40	1.13	0.88	0.92	1.29	53/142	05/282	52/018	37/188
LC3	1.14	36	1.20	45	1.23	64	1.20	0.91	2.03	1.32	56/136	25/284	28/029	50/159
LC4	1.05	174	1.06	77	1.13	92	1.06	0.94	0.83	1.13	67/124	53/302	13/050	34/149
LC5	1.16	1	1.20	37	1.02	74	1.03	0.84	0.16	1.22	30/178	08/277	13/009	75/156
LC6	1.15	165	1.20	30	1.21	28	1.15	0.89	1.23	1.29	30/178	25/296	29/040	51/172
LC7	1.29	16	1.21	23	1.07	50	1.12	0.84	0.62	1.33	30/178	14/288	13/022	71/154
LC8	1.15	54	1.31	106	1.34	50	1.22	0.81	0.96	1.50	76/346	48/113	37/258	18/002
LC9	1.13	66	1.27	68	1.25	49	1.19	0.86	1.16	1.38	90/340	07/280	71/031	17/188
LC10	1.19	49	1.20	55	1.20	107	1.12	0.84	0.64	1.33	90/318	47/278	16/026	38/129
LC11	1.06	110	1.27	70	1.26	81	1.04	0.80	0.14	1.30	74/298	68/278	11/035	19/129
LC12	1.15	75	1.20	80	1.21	93	1.10	0.88	0.70	1.26	80/304	64/277	13/035	22/130
LC13	1.19	85	1.22	78	1.18	105	1.13	0.88	0.94	1.28	64/306	48/279	22/035	34/141
LC14	1.07	155	1.21	69	1.15	78	1.02	0.84	0.09	1.21	83/327	48/271	37/061	16/163

A, B, and C = three mutually perpendicular sections; R_f = axial ratio of the ellipse; ϕ = orientation of the ellipse from the horizontal reference line (CCW positive); 3-D principal strain ratios (S_1/S_2 and S_2/S_3) are calculated from 2-D strain values of A, B, and C; k = Flinn value; S_1/S_3 = axial ratio of 3-D strain ellipsoid; Bedding = bedding orientation; E_1, E_2, and E_3 represent the orientations of principal axes in geographic reference frame.

In the absence of any metamorphic indicators we have used the dominant deformation mechanisms in quartz-rich rocks to obtain estimates of the thermal history of deformation (Mitra, 1997; Ismat and Mitra, 2005). The presence of early plastic deformation features indicates deformation temperatures greater than the elastico-frictional–quasi-plastic transition for quartz (Sibson, 1977), i.e. $T > 300$ °C with corresponding depths of 10–12 km (at typical hinterland geothermal gradients of 25–30 °C/km; Smith and Bruhn, 1984). Late stage cataclastic deformation took place at shallower depths (above the EF–QP transition) with estimated depths of 2–5 km based on thickness of synorogenic overburden in the Canyon Range thrust sheet (Ismat and Mitra, 2005). We interpret the overprinting of crystal plastic microstructures by cataclastic features to be a result of the rocks being brought closer to the surface due to uplift and erosion during progressive deformation. This microstructural interpretation is consistent with our thrust fault interpretation of the Leamington Canyon thrust based on kinematic analysis and structural geometry.

5. 3-D kinematic analysis at an oblique ramp

Kinematic analysis included (1) determining maximum stretching directions of finite strain ellipsoids for quartzite samples (Anderson, 1948; Flinn, 1956; Hossack, 1968, 1978; Wood, 1973; Chapman et al., 1979; McNaught and Mitra, 1996), (2) determining M poles for fracture populations with slickenlines (Arthaud, 1969; Wojtal, 1982; Alexandrowski, 1985; Goldstein and Marshak, 1988; Mitra, 1993), and (3) determining maximum shortening directions from orientations of conjugate–conjugate fracture sets (Reches, 1978; Ismat and Mitra, 2000). From the available local relative timing information and microstructural studies (described above), we interpret that these microscopic and outcrop scale structures were formed at different depths, and represent different stages of deformation as the rocks were brought closer to the surface by uplift and erosion during progressive deformation. The use of these three methods allows comparison of superimposed deformation phases during thrust sheet emplacement.

5.1. 3-D strain analysis

The Leamington Canyon thrust sheet is dominated by Proterozoic ('Pocatello', Caddy Canyon and Mutual Formations) and early Cambrian (Tintic Formation) quartzites, which allow finite strain to be determined using the Fry method (Fry, 1979; Erslev, 1988; Erslev and Ge, 1990; McNaught, 1994; Mukul and Mitra, 1998b). These strains represent an early increment of deformation when the rocks were sufficiently deep to have undergone 'crystal plastic' deformation; we estimate a depth of more than ~10 km overburden from a stratigraphic package of Precambrian Caddy Canyon Formation to Permian Park City Formation (Kwon and Mitra, 2005), and assume a hinterland geothermal gradient of ~26 °C/km, equivalent to the present-day gradient (Smith and Bruhn, 1984) as an example. This early increment of deformation typically involves layer-parallel shortening

followed by bedding parallel shear (Gray and Mitra, 1993; Mukul and Mitra, 1998b). To determine 3-D strains, systematic oriented samples were colleted from Proterozoic to early Cambrian hanging wall quartzites of the Leamington Canyon thrust along the Leamington zone. Strain ellipses were determined using the modified normalized center-to-center Fry technique (McNaught, 1994) for each sample. These section ellipses from three mutually perpendicular sections were then used to define best-fit 3-D ellipsoids following the method outlined by Strine (www.earth.rochester.edu/structure/matty/main.html). The 2-D strain magnitudes and orientations (input data) from three mutually perpendicular thin sections and the 3-D strain results are reported in Table 1. The finite strain ellipsoids, long-axis orientations (E_1), Flinn (k)-values, and S_1/S_3 (long-axis/short-axis) axial ratios are shown in Fig. 11. Because the measured finite strain ellipsoids give the earliest kinematic information for each area, the long-axis orientations (E_1) were used to estimate the earliest stage kinematic directions in terms of maximum stretching directions at the Leamington zone. Long-axis orientations of finite strain ellipsoids (Fig. 11) trend E–ESE (91–122°) and plunge 8–68° to the WNW, and the S_1/S_3 axial ratios range from 1.13

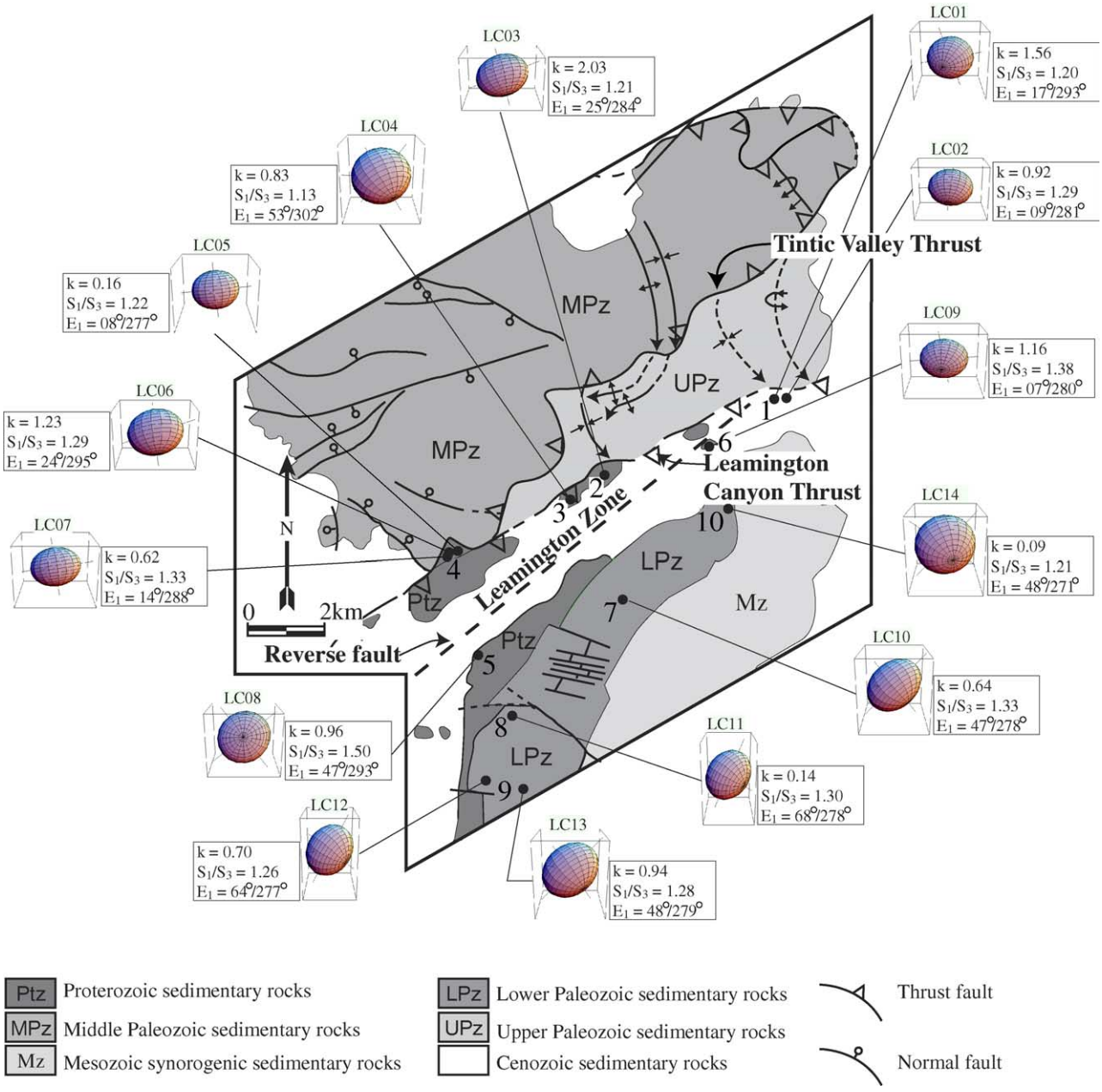

Fig. 11. Generalized geologic map of the Leamington zone area showing locations for 3-D grain-scale plastic strain analyses. The strain ellipsoids were measured from mutually perpendicular thin sections following the methods of Strine (www.earth.rochester.edu/structure/matty/maim.html). Numbers with filled circles indicate the locations of kinematic analyses. The k-values, S_1/S_3 ratios and E_1 orientations represent the shape of the ellipsoids, axial ratios (long-axis/short-axis) of the ellipsoids, and plunge and trend of the ellipsoid long-axes, respectively.

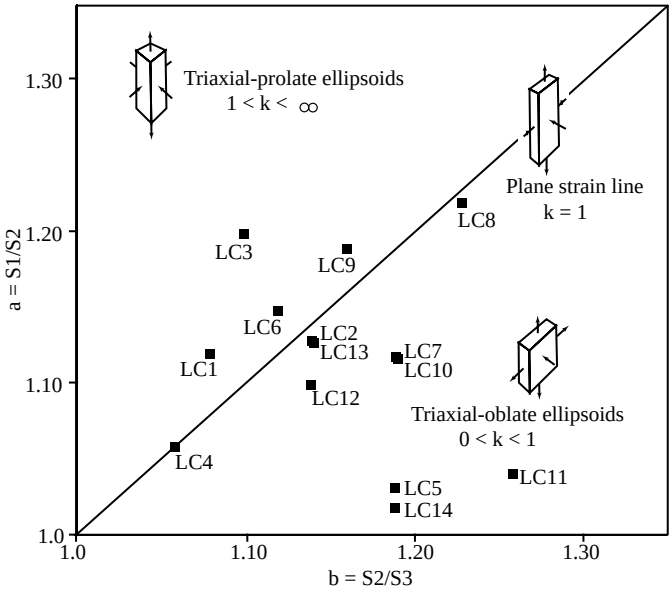

Fig. 12. Flinn diagram showing shapes of the strain ellipsoids from the hanging wall quartzites of the Leamington Canyon thrust.

to 1.50. A Flinn diagram of the 3-D finite strain data from the Leamington zone shows that most of the ellipsoids plot in the triaxial-prolate to triaxial-oblate fields close to the line of apparent plane strain (Fig. 12). The dominant triaxial-oblate strain in three samples may reflect the uncertainties that are caused from primary sedimentary fabrics.

5.2. Fracture analyses (M-plane and conjugate–conjugate fracture sets)

Fracture populations that developed during the formation of the Leamington Canyon thrust form a penetrative deformation fabric at the outcrop scale, and can be used to determine overall shortening directions (e.g. Arthaud, 1969) for each stage of deformation (Ismat and Mitra, 2000). In the Leamington zone area, two types of fracture populations (i.e. fractures with slickenlines, and uncemented fractures) are prominently observed at an outcrop scale. Cross-cutting relationships suggest that the fractures with slickenlines are older than the uncemented fractures; the latter occur in conjugate–conjugate sets and show mutually cross-cutting relationships. We determined the azimuth of the motion plane and the maximum shortening direction for the earlier deformation phase from fracture populations with slickenlines using M-plane analysis. The method of acute bisector of the conjugate–conjugate uncemented fracture sets (Reches, 1978, 1983; Ismat and Mitra, 2000, 2005) was used to infer maximum shortening directions for the last phase of contractional deformation.

Successive generations of fractures can be distinguished from their microscopic (Sussman, 1995) and outcrop scale characteristics, cross-cutting relationships and degree of reactivation (Ismat and Mitra, 2000). In the areas of the Leamington zone, the fractures with slickenlines are the older fractures observed at the outcrop scale. Microscopic cross-cutting relationships suggest that these fractures formed later than the plastic microstructures (e.g. intragranular cracks, undulose extinction and deformation bands) and strains, indicating that they developed as the rocks were brought closer to the surface by uplift and erosion during progressive emplacement of the Leamington Canyon thrust sheet. If insufficient information from cross-cutting relationships was available, we used the most prominent fractures as the youngest, based on Ismat and Mitra (2000); thus the prominent uncemented fractures observed at an outcrop scale are younger than the fractures with slickenlines. These late uncemented fractures are probably related with folding and subsequent fold-tightening of the Leamington Canyon thrust by cataclastic flow, caused by the formation of underlying structures (e.g. Tintic Valley thrust and Jericho horse) in a manner similar to the Canyon Range syncline to the south (Ismat and Mitra, 2000, 2005). Therefore, kinematic directions for three different stages of deformation over the oblique ramp can be determined from these relationships.

A total of 10 stations were considered in detail (Figs. 11 and 13). In four of them, three different directions were measured from the methods below. In the other six, only the first and last stage directions were measured because of the lack of fractures with slickenlines away from the fault (Area 5-10 of Fig. 13).

The maximum stretching direction determined from the azimuth of the long-axis orientation of the 3-D plastic strain trend 91–122° (Fig. 13) and represents the earliest stage (stage 1); the direction of motion from fracture populations with slickenlines using M-plane analysis trend 134–152° (Fig. 13) and gives the second stage (stage 2); and the maximum shortening directions from the orientations of the acute bisector of conjugate–conjugate fracture sets from late (uncemented) fractures shows even more southward directions of 142–180° (Fig. 13) and indicates the latest stage (stage 3).

Therefore, results of kinematic analyses from the three observed stages of superimposed deformation together with

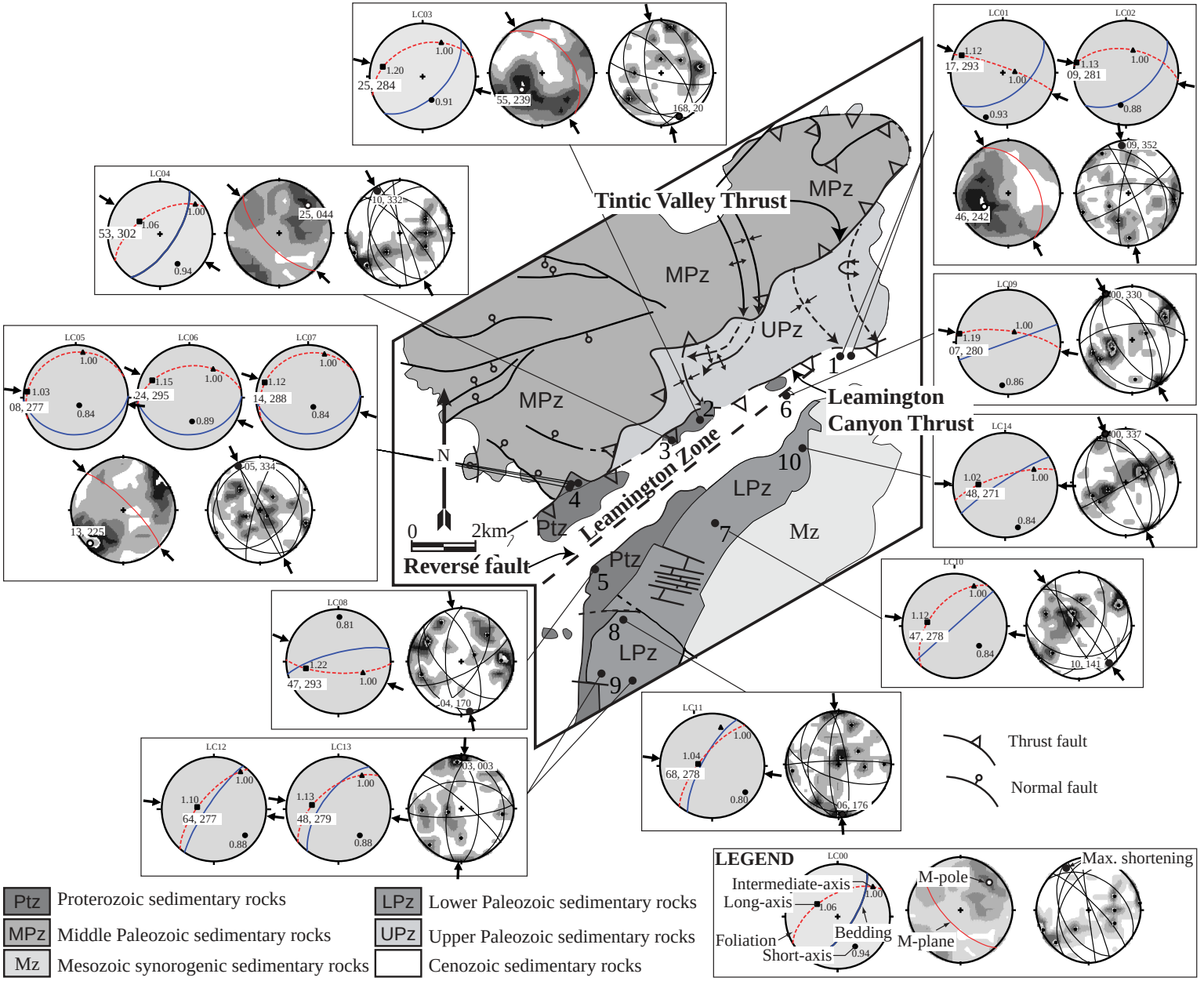

Fig. 13. Generalized geologic map of the Leamington zone area showing locations for kinematic analyses of different stages. The long-axis orientations of strain ellipsoids are the earliest stage: long-axis orientation and relative strain magnitudes are indicated by numbers at each axis; the trace of bedding and grain shape foliation are also shown by solid and dotted line great circles, respectively. The azimuth of motion planes from fractures with slickenlines (by M-plane analysis) is the second stage. Maximum shortening directions from populations of late fractures (using acute bisector of conjugate–conjugate sets) are the latest stage. Large black arrows indicate local kinematic directions for each stage of deformation.

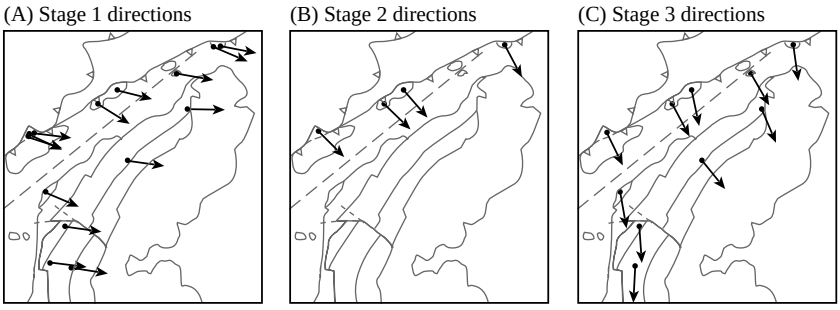

Fig. 14. Maps showing the results of kinematic analyses at the Leamington Zone. Arrows indicate kinematic directions for each stage of deformation. Stage 1 directions (maximum stretching directions) are estimated from the azimuth of the long-axis orientation of the 3-D plastic strain. Stage 2 directions (fault motion directions) are determined from fracture populations with slickenlines using M-plane analysis. Stage 3 directions (maximum shortening directions) are inferred from the orientations of the acute bisector of conjugate–conjugate fracture sets from late fractures (with mutual cross-cutting relationships).

local relative chronologies (from cross-cutting relationships) between plastic and brittle structures demonstrate that the local kinematic directions changed about a vertical-axis from E- to ESE- to SSE-directions during successive pulses of deformation along the Leamington zone (Fig. 14); meanwhile the regional kinematic directions (in the Sevier fold–thrust belt as a whole) maintained an E–W trend.

6. Discussion

6.1. Implication of temporal change in kinematic directions at an oblique transverse zone and insights from mechanical and kinematic studies

The results from 3-D strain studies demonstrate that the ellipsoid long-axis orientations show dominant E- to ESE-stretching directions (Figs. 11 and 13). To eliminate the effects of folding in the Leamington zone area, stage 1 local directions were unfolded about a fold-axis (30°, 235°) of the Leamington oblique transverse zone. The results show similar E- to ESE-directions of 94–131°, with an average stage 1 direction of 120°. The stage 2 directions (134–152°) also show similar SE directions (130–156°) after unfolding. The stage 3 direction is not considered because the late (open) fractures are formed during folding and fold-tightening of the Leamington Canyon thrust by later emplacement of underlying younger structures (e.g. Tintic Valley thrust and Jericho horse). Results indicate that stage 1 and 2 directions were not significantly affected by folding about a gentle SW fold-axis. Thus, either kinematic directions changed or earlier fabrics underwent vertical-axis rotations during progressive deformation along the Leamington zone.

The Leamington zone area may have undergone fold-tightening by cataclastic flow like the Canyon Range syncline to the south (Ismat and Mitra, 2000, 2005). During this deformation, the oblique ramp area may have experienced local vertical-axis rotations caused by block rotations during folding and fold-tightening by emplacement of underlying younger structures (e.g. Tintic Valley thrust and Jericho horse) as shown in stepwise restorations (Fig. 8). If the observed changes in local kinematic directions were entirely a result of block rotations, then stage 1 directions would have been rotated passively during folding and subsequent fold-tightening by cataclastic flow. However, (1) consistent bedding orientations are preserved irrespective of block rotations indicating that local vertical-axis rotations are actually small, and (2) the stage 1 directions did not passively rotate to the same orientations as the latest stage (stage 3) directions derived from conjugate–conjugate fracture sets. Thus, the 3-D finite strain ellipsoids represent the true orientations of an early increment of deformation (possibly with small amounts of local vertical-axis rotations). These arguments also hold for the second stage (stage 2) directions from M-plane analysis. Thus, the changes in directions observed along the Leamington zone partly reflect superimposed deformations during successive pulses of deformation, with small amounts of local vertical-axis rotations during later folding and fold-tightening of the Leamington Canyon thrust. Although our qualitative interpretations of changing kinematic patterns during progressive deformation may be reasonable, quantitative estimates of components of vertical-axis rotations probably require additional data.

From previous work on mechanical and kinematic models for oblique ramps, at least two possible causes may explain the interpreted temporal changes in local kinematic directions in the study area: (1) clockwise changes in stress orientation due to interaction between the transport-parallel motion of the wedge and the pre-existing oblique ramp structure, as indicated by mechanical and analytical models (Casas et al., 1992; Apotria, 1995); and (2) vertical-axis block rotation (Bates, 1989; McCaig and McClelland, 1992) during folding and fold-tightening of the Leamington zone.

Mathematical simulation of stress trajectories at an oblique ramp using 2-D finite element modeling (Casas et al., 1992) shows the tendency of the σ_1 trajectory to become perpendicular to the strike of the oblique ramp. Apotria (1995) also showed, in his analytical model based on 3-D continuum mechanics, that the maximum principal stress and strain rates occur in a plane perpendicular to the oblique ramp strike. If we assume these results as the maximum possible changes in stage 3 local directions at an oblique ramp, then the minimum amounts of vertical-axis block rotation can be calculated. As

described in the section on kinematic analysis, the average stage 3 kinematic direction, from populations of late (uncemented) fractures, along the Leamington zone is 162°. Therefore, the estimated minimum amount of vertical-axis rotation by cataclastic flow during fold tightening is a clockwise rotation of 12° with respect to the dip direction (150°) of the Leamington Canyon thrust.

From the above discussion, there are a minimum of two possible stages of superimposed deformation over the oblique ramp during progressive deformation. During the earliest stage, due to interaction of the overall easterly displaced wedge with the oblique ramp structure, the kinematic directions (fault motion and maximum shortening directions) over the oblique ramp become perpendicular to the strike of the Leamington Canyon thrust (NW–SE); this agrees with the direction of maximum principal stress as indicated by kinematic and mechanical models (Casas et al., 1992; Apotria, 1995). During the two later stages, the SE-kinematic directions are rotated further southward by local block rotations (Bates, 1989; McCaig and McClelland, 1992) during folding and subsequent fold tightening of the Leamington Canyon thrust.

6.2. Implications for salient formation from the kinematic history at an oblique transverse zone

The observed kinematic history along the Leamington zone has ramifications for the evolution of the Provo salient. Because of (1) the existence of old sedimentary basin boundaries that served as transverse zones at both the northern (Charleston transverse zone) and the southern ends, and (2) the close relationship between the pre-deformational basin-geometry and the arcuate shape (Macedo and Marshak, 1999), the initial orogenic wedge of the Provo salient probably developed as a three-dimensionally tapered wedge (Gray and Mitra, 1993; Gray and Stamatakos, 1997).

The overall W–E stage 1 maximum stretching directions, determined from the azimuth of strain ellipsoid long-axis orientations, represent an early increment of deformation, which probably developed at the rear of the 3-D wedge as it proceeded from the hinterland towards the foreland.

As the 3-D wedge migrated eastward toward the foreland, it interacted with a pre-existing oblique ramp structure to generate maximum shortening directions perpendicular to the strike of the oblique ramp as indicated by kinematic and mechanical models (Casas et al., 1992; Apotria, 1995). The maximum shortening direction at this stage was recorded in the form of lower temperature deformation structures (e.g. fractures) because the rocks were brought progressively closer to the surface by uplift and erosion during progressive deformation. Evidence for this progressive unroofing is seen in the form of overprinting microstructures formed at successively lower *P–T* conditions (Fig. 10). For the Provo salient as a whole, the mesoscopic structures preserve evidence for clockwise changes in kinematic directions from eastward to southeastward directions along the Leamington zone, while the overall kinematic direction at the frontal ramp was still in the overall W–E regional transport direction (Allmendinger, 1992; Constenius, 1998).

The Leamington zone area experienced further small amounts of vertical-axis rotation of kinematic direction from SE to SSE by block rotations due to folding and subsequent fold tightening by cataclastic flow (Ismat and Mitra, 2000) during the formation of underlying structures (e.g. Tintic Valley thrust and Jericho horse).

In fold–thrust belts it is generally assumed that there is no significant motion of material in-and-out of a line of cross-section parallel to the regional transport direction and that deformation takes place by plane strain. The observed changes in kinematics at the Leamington zone clearly show that these fundamental assumptions of balanced cross-sections are not valid at the ends of a salient. The assumptions break down when thrust sheets undergo changes in kinematic directions by interaction with transverse structures and in these situations the deformation is clearly non-plane strain. For rigorous treatment of such structures, where the total deformation is being determined by components of forward motion and lateral variations in structural geometry, the overall deformation would be better studied in three dimensions.

7. Conclusions

1. Map patterns, stratigraphic-separation diagrams, kinematic indicators, down-plunge projection and microstructures all suggest that the Leamington Canyon thrust is a folded thrust fault, with top-down to the southeast shear.
2. The Leamington transverse zone consists of the folded Leamington Canyon thrust, associated folds and an out-of-syncline reverse fault. The folded Leamington Canyon thrust is essentially the same fault as the folded Canyon Range thrust, and serves not only as an oblique ramp of the folded Canyon Range thrust to the south, but also as a termination for the Tintic Valley thrust to the north. Emplacement of the Tintic Valley thrust and the underlying Jericho horse caused fold tightening of the syncline in front of the folded Leamington Canyon thrust. This fold tightening took place within the elastico-frictional regime by cataclastic flow (Ismat and Mitra, 2000) and caused out-of-syncline reverse faulting in the fold core. Overall, the Leamington zone serves as a complex slip accommodation zone at the boundary between two prominent segments (namely the Provo salient and the Central Utah segment) of the Sevier fold–thrust belt.
3. Three different methods were used for inferring the 3-D kinematic history at an oblique ramp along the Leamington zone. Based on the results of superimposed deformation from kinematic analyses together with local relative chronologies, we determined the temporal changes in kinematic directions over the oblique ramp from E- to SE- to SSE-directions during successive pulses of deformation. The restored eastward kinematic directions, inferred from the maximum stretching directions of the 3-D strain ellipsoid long-axis orientations, are the earliest stage (stage 1). The SE-directions, inferred from the azimuth of

motion plane using M-plane analysis from fractures with slickenlines, are the second stage (stage 2). And the SSE-directions, determined from the maximum shortening directions using the method of acute bisectors of conjugate–conjugate late fracture sets, are the latest stage (stage 3).

4. The observed clockwise changes in kinematic direction along the Leamington zone most likely reflect temporal variations in kinematics over the oblique ramp as the easterly displaced 3-D fold–thrust belt wedge interacted with a pre-existing oblique ramp structure. There were small amounts of superimposed local vertical-axis rotations during later folding and fold-tightening of the Leamington Canyon thrust.

Acknowledgements

This work was supported by National Science Foundation grant EAR-0208001 to G. Mitra and by grants from the Geological Society of America and the Nuria Pequera Fellowship of the University of Rochester to S. Kwon. This paper represents part of SK's Ph.D. research performed at the University of Rochester. Constructive reviews by A. Yonkee, D. Wise and T. Apotria, and editorial suggestions by D.A. Ferrill led to considerable improvement of the final manuscript. Stereograms and best-fit ellipsoids used in the paper were generated using Richard Allmendinger's "Stereonet," and Matty Strine's "strain ellipsoid program", respectively.

References

Alexandrowski, P., 1985. Graphical determination of principal stress directions for slickenside lineation populations: an attempt to modify Arthaud's method. Journal of Structural Geology 7, 73–82.

Allmendinger, R.W., 1992. Fold and thrust tectonics of the western United States exclusive of the accreted terranes. In: Burchfiel, B.C., Lipman, P.W., Zoback, M.L. (Eds.), The Cordilleran Orogen, the Conterminous U.S. Geological Society of America, The Geology of North America G-3, pp. 583–608.

Allmendinger, R.W., Sharp, J.W., Von Tish, D., Serpa, L., Brown, L., Oliver, J., Kaufman, S., Smith, R.B., 1983. Cenozoic and Mesozoic structure of the eastern Basin and Range province, Utah, from COCORP seismic reflection data. Geology 11, 532–536.

Anderson, E.M., 1948. On lineation and petrofabric structure, and the shearing movement by which they have been produced. Quarterly Journal of Geological Society London 54, 99–126.

Apotria, T.G., 1995. Thrust sheet rotation and out-of-plane strains associated with oblique ramps: an example from the Wyoming salient, U.S.A. Journal of Structural Geology 17, 647–662.

Armstrong, R.L., 1968. Sevier orogenic belt in Nevada and Utah. Geological Society of America Bulletin 79, 429–458.

Arthaud, F., 1969. Methode de determination graphique des directions de raccoureissement, d'allongement et intermediaire d'une population de dailles. Compte Rendu Sommaire des séances de la Cociete Geologique de France 8, 302.

Ashby, M.F., Grandhi, C., Taplin, D.M.R., 1979. Fracture mechanism maps and their construction for F.C.C. metals and alloys. Acta Metallurgica 27, 699–729.

Bates, M.P., 1989. Paleomagnetic evidence for rotations and deformation in the Nogueras Zone, Central Southern Pyrenees, Spain. Journal of Geological Society London 146, 459–476.

Black, B.A., 1965. Nebo overthrust, southern Wasatch Mountains, Utah. Brigham Young University Geologic Studies 12, 55–89.

Bruhn, R.L., Picard, M.D., Isby, J.S., 1986. Tectonics and sedimentology of the Uinta Arch, western Uinta Mountains, and Uinta Basin. In: Peterson, J.A. (Ed.), Paleotectonics and Sedimentation in the Rocky Mountain Region, United States. American Association of Petroleum Geology Memoir 41, pp. 119–141.

Burchfiel, B.C., Davis, G.A., 1975. Nature and controls of Cordilleran orogenesis, western United States—extensions of an earlier synthesis. American Journal of Science 275A, 363–396.

Burchfiel, B.C., Hickcox, C.W., 1972. Structural development of central Utah. In: Baer, J.L., Callaghan, E. (Eds.), Plateau-Basin and Range Transition Zone, Central Utah. Utah Geological Association Publication 2, pp. 55–66.

Casas, A.M., Simon, J.L., Seron, F.J., 1992. Stress deflection in a tectonic compressional field: a model for the northeastern Iberian Chain, Spain. Journal of Geophysical Research 97, 7183–7192.

Chapman, T.G., Milton, N.J., Williams, G.D., 1979. Shape fabric variations in deformed conglomerates at the base of the Laksefjord Nappe, Norway. Journal of Geological Society, London 136, 683–691.

Christiansen, R.F., 1952. Structure and stratigraphy of the Canyon Range, Utah. Geological Society of America Bulletin 63, 717–740.

Christie-Blick, N.H., 1983. Structural geology of the southern Sheeprock Mountains, Utah: regional significance. In: Miller, D.M., Todd, R., Howard, K.A. (Eds.), Tectonics and Stratigraphic Studies in the Eastern Great Basin. Geological Society of America Memoir 157, pp. 101–124.

Constenius, K.N., 1996. Late Paleogene extensional collapse of the Cordilleran foreland fold and thrust belt. Geological Society of America Bulletin 108, 20–39.

Constenius, K.N., 1998. Extensional tectonics of the Cordilleran fold–thrust belt and the Jurassic–Cretaceous Great Valley forearc basin. Ph.D. dissertation, University of Arizona, 232pp.

Coogan, J.C., DeCelles, P.G., Mitra, G., Sussman, A.J., 1995. New regional balanced cross section across the Sevier desert region and the Central Utah thrust belt. Geological Society of America Rocky Mountain Section Meeting Abstracts 27, 7.

Costain, J.K., 1960. Geology of the Gilson Mountains and vicinity, Juab County, Utah. Ph.D. dissertation, University of Utah, Salt Lake City, 178pp.

DeCelles, P.G., Mitra, G., Lawton, T.F., 1993. The Canyon Range Culmination, central Utah Sevier thrust belt: long term control on synorogenic sedimentation in Cordilleran foreland basin. Geological Society of America Annual Meeting Abstracts 25, A174.

DeCelles, P.G., Lawton, T.F., Mitra, G., 1995. Thrust timing, growth of structural culminations, and synorogenic sedimentation in the type Sevier orogenic belt, western United States. Geology 23, 699–702.

Erslev, E.A., 1988. Normalized center-to-center strain analysis of packed aggregates. Journal of Structural Geology 10, 201–209.

Erslev, E.A., Ge, H., 1990. Least-squares center-to-center and mean object ellipse fabric analysis. Journal of Structural Geology 12, 201–209.

Flinn, D., 1956. On the deformation of the Funzie conglomerate, Fetlar, Shetland. Journal of Geology 64, 480–505.

Fry, N., 1979. Random point distribution and strain measurement in rocks. Tectonophysics 60, 89–105.

Goldstein, A., Marshak, S., 1988. Analysis of fracture array geometry. In: Marshak, S., Mitra, G. (Eds.), Basic Methods of Structural Geology. Prentice Hall, Englewood Cliffs, New Jersey, pp. 249–268.

Gray, M.B., Mitra, G., 1993. Migration of deformation fronts during progressive deformation: evidence from detailed structural studies in the Pennsylvania Anthracite region, U.S.A. Journal of Structural Geology 15, 435–449.

Gray, M.B., Stamatakos, J., 1997. New model for evolution of fold and thrust belt curvature based on integrated structural and paleomagnetic results from the Pennsylvania salient. Geology 25, 1067–1070.

Higgins, J.M., 1982. Geology of the Champlin Peak quadrangle, Juab and Millard counties, Utah. Brigham Young University Geology Studies 29, 40–58.

Hintze, L.F., 1988. Geologic history of Utah. Brigham Young University Geology Studies Special Publication 7, 202pp.

Holladay, J.C., 1983. Geology of the northern Canyon Range, Millard and Juab counties, Utah. Brigham Young University Geology Studies 31, 1–28.

Hossack, J.R., 1968. Pebble deformation and thrusting in the Bygdin area (Southern Norway). Tectonophysics 5, 315–339.

Hossack, J.R., 1978. The correction of stratigraphic sections for tectonic finite strain in the Bygdin area, Norway. Journal of Geological Society, London 136, 705–712.

Ismat, Z., Mitra, G., 2000. Folding by cataclastic flow at shallow crustal levels in the Canyon Range, Sevier orogenic belt, west-central Utah. Journal of Structural Geology 23, 355–373.

Ismat, Z., Mitra, G., 2005. Fold–thrust belt evolution expressed in an internal thrust sheet, Sevier orogen: the role of cataclastic flow. Geological Society of Bulletin 117, 764–782.

Kulik, D.M., Schmidt, C.J., 1988. Region of overlap and styles of interaction of Cordilleran thrust belt and Rocky Mountain foreland. Geological Society of America Memoir 171, 75–98.

Kwon, S., Mitra, G., 2001. The geometry, kinematics and deformation characteristics of the Leamington Canyon transverse zone, central Utah. Geological Society of America Annual Meeting Abstract 33 (6), A149–A150.

Kwon, S., Mitra, G., 2004. Strain distribution, strain history and kinematic evolution associated with the formation of arcuate salients in fold–thrust belts: the example of the Provo salient, Sevier orogen, Utah. In: Sussman, A., Weil, A. (Eds.), Orogenic Curvature Geological Society of America Special Paper 383-14, pp. 205–223.

Kwon, S., Mitra, G., 2005. Provisional structural geologic map of the Jericho Quadrangle, Juab County, Utah. Utah Geological Survey Open File Report 444 25pp. with 2 plates, scale 1:24,000.

Lageson, D.R., Schmitt, J.G., 1995. The Sevier orogenic belt of the western United States: recent advances in understanding its structural and sedimentological framework. In: Caputo, M.P., Peterson, J.A., Franczyk, K.J. (Eds.), Mesozoic Systems of the Rocky Mountain Region U.S.A. Rocky Mountain Section SEPM, Denver, CO, pp. 27–64.

Lawton, T.F., 1982. Lithofacies correlations within the Upper Cretaceous Indianola Group. In: Nielson, D.L. (Ed.), Overthrust Belt of Utah. Utah Geological Association Publication 10, pp. 199–213.

Lawton, T.F., 1985. Style and timing of the frontal structures, Sevier thrust belt, central Utah. American Association of Petroleum Geology Bulletin 69, 1145–1159.

Lawton, T.F., Boyer, S.E., Schmitt, J.G., 1994. Influence of inherited taper on structural variability and conglomerate distribution, Cordilleran fold and thrust belt, western United States. Geology 22, 339–342.

Lawton, T.F., Sprinkel, D.F., DeCelles, P.G., Mitra, G., Sussman, A.J., Weiss, M.P., 1997. Sevier thrust belt central-Utah: Sevier Desert to Wasatch Plateau. In: Link, K.P., Kowallis, B.J. (Eds.), Brigham Young University Geology Studies Field Trip Guide Book, pt. 2. Geological Society of America Annual Meeting, pp. 33–68.

Levy, M., Christie-Blick, N., 1989. Pre-Mesozoic palinspastic reconstruction of the eastern Great Basin (western United States). Science 245, 1454–1462.

Mabey, D.R., Morris, H.T., 1967. Geologic interpretation of gravity and aeromagnetic maps of Tintic Valley and adjacent areas, Toole and Juab countries, Utah. U.S. Geological Survey Professional Paper 516-D, 1–10.

Macedo, J., Marshak, S., 1999. Controls on the geometry of fold–thrust belt salients. Geological Society of America Bulletin 111, 1808–1822.

Marshak, S., 1988. Kinematics of orocline and arc formation in thin-skinned orogens. Tectonics 7, 73–86.

McCaig, A.M., McClelland, E., 1992. Paleomagnetic technique applied to thrust belts. In: McClay, K.R. (Ed.), Thrust Tectonics. Chapman & Hall, London, pp. 209–216.

McNaught, M.A., 1994. Modifying the normalized Fry method for aggregates of non-elliptical grains. Journal of Structural Geology 18, 573–583.

McNaught, M.A., Mitra, G., 1993. A kinematic model for the origin of footwall synclines. Journal of Structural Geology 15, 805–808.

McNaught, M.A., Mitra, G., 1996. The use of finite strain data in constructing a retrodeformable cross-section of the Meade thrust sheet, southeastern Idaho. Journal of Structural Geology 16, 493–503.

Millard Jr., A.W., 1983. Geology of the southwestern quarter of the Scipio North (15-minute) quadrangle, Millard and Juab counties Utah. Brigham Young University Geology Studies 30, 59–81.

Miller, D.M., Nilsen, T.H., Bilodeau, W.L., 1992. Late Cretaceous to early Eocene geologic evolution of the U.S. Cordillera. In: Burchfiel, B.C., Lipman, P.W., Zoback, M.L. (Eds.), The Cordilleran Orogen, the Conterminous U.S. Geological Society of America, The Geology of North America G-3, pp. 205–260.

Mitra, G., 1978. Ductile deformation zones and mylonites: the mechanical processes involved in the deformation of crystalline basement rocks. American Journal of Science 278, 1057–1084.

Mitra, G., 1984. Brittle to ductile transition due to large strains along the White Rock thrust, Wind River Mountains, Wyoming. Journal of Structural Geology 6, 51–61.

Mitra, G., 1993. Deformation processes in brittle deformation zones in granitic basement rocks: a case study from the Torry Creek area, Wind River Mountains. Geological Society of America Special Paper 280, 177–195.

Mitra, G., 1997. Evolution of salients in a fold-and-thrust belt: the effects of sedimentary basin geometry, strain distribution and critical taper. In: Sengupta, S. (Ed.), Evolution of Geological Structures from Macro- to Micro-scales. Chapman and Hall, London, pp. 59–90.

Mitra, G., Sussman, A.J., 1997. Structural evolution of connecting splay duplexes and their implications for critical taper: an example based on geometry and kinematics of the Canyon Range culmination, Sevier Belt, central Utah. Journal of Structural Geology 19, 503–521.

Mitra, G., Pequera, N., Sussman, A.J., DeCelles, P.G., 1994. Evolution of structures in the Canyon Range thrust sheet (Sevier fold-and-thrust belt) based on field relations and microstructural studies. Geological Society of America Annual Meeting Abstracts 26, A527.

Mitra, G., Sussman, A.J., Pequera, N., DeCelles, P.G., Coogan, J.C., 1995. Structural evolution of the Canyon Range, Central Utah Sevier orogenic wedge: implications for critical taper during thrusting. Geological Society of America Rocky Mountain Section Meeting Abstracts 27, 47.

Morris, H.T., 1983. Interrelations of thrust and transcurrent faults in the central Sevier orogenic belt near Leamington, Utah. Geological Society of America Memoir 157, 75–81.

Morris, H.T., Kopf, R.W., 1969. Tintic Valley thrust and associated low-angle faults, central Utah. Geological Society of Annual Meeting Abstracts, 55–56.

Morris, H.T., Lovering, T.S., 1979. General geology and mines of the East Tintic Mountains, Utah. U.S. Geological Survey Professional Paper 501-C, C19–C21.

Morris, H.T., Shepard, W.M., 1964. Evidence for a concealed tear fault with large displacement in the central East Tintic Mountains, Utah: new interpretations based on structural analysis. Geological Society of America Rocky Mountain Section Meeting Abstracts 26, 55.

Mukul, M., Mitra, G., 1998a. Stratigraphy and structural geology of the southern Sheeprock and the adjacent West Tintic Mountains (Utah): a review and new interpretations based on structural analysis. Utah Geological Survey Miscellaneous Publications 98-1, 17–56.

Mukul, M., Mitra, G., 1998b. Finite strain and strain variation analysis in the Sheeprock thrust sheet, an internal thrust sheet in the Provo salient of the Sevier fold-and-thrust belt, central Utah. Journal of Structural Geology 20, 385–406.

Pampeyan, E.H., 1989. Geologic map of the Lynndyl 30- by 60-minute quadrangle, west central Utah. U.S. Geological Survey Miscellaneous investigation series Map I-1830.

Passchier, C.W., Trouw, R.A.J., 1996. Microtectonics. Springer, Berlin. 289pp.

Paulsen, T., Marshak, S., 1997. Structure of the Mount Raymond transverse zone at the southern end of the Wyoming salient, Sevier fold-thrust belt, Utah. Tectonophysics 280, 199–211.

Paulsen, T., Marshak, S., 1999. Origin of the Uinta recess, Sevier fold-thrust belt, Utah: influence of basin architecture on fold-thrust belt geometry. Tectonophysics 312, 203–216.

Pequera, N., Mitra, G., Sussman, A.J., 1994. The Canyon Range thrust sheet in the Sevier fold-and-thrust belt of central Utah: deformation history based on structural analysis. Geological Society of America Rocky Mountain Section Meeting Abstracts 26, 58.

Peterson, J.A., 1977. Paleozoic shelf margins and marginal basins, western Rocky Mountains-Great Basin, United States. In: Hesley, E.L. et al. (Ed.), Rocky Mountain Thrust Belt, Geology and Resources Guidebook. Wyoming Geological Association Annual Field Conference 29, pp. 135–153.

Reches, Z., 1978. Analysis of faulting in three-dimensional strain field. Tectonophysics 47, 109–129.

Reches, Z., 1983. Faulting of rocks in three-dimensional strain fields: II. Theoretical analysis. Tectonophysics 95, 133–156.

Royse, F., 1993. Case of the phantom foredeep: Early Cretaceous in west central Utah. Geology 21, 41–45.

Schwartz, R.K., DeCelles, P.G., 1988. Cordilleran foreland-basin evolution and synorogenic sedimentation in response to interactive Cretaceous thrusting and reactivated foreland partitioning. In: Schmidt, C.J., Perry, W.J. (Eds.), Interaction of the Rocky Mountain Foreland and Cordilleran Thrust Belt. Geological Society of America Memoir 171, pp. 489–514.

Sibson, R.H., 1977. Fault rocks and fault mechanisms. Journal of the Geological Society of London 133, 191–213.

Smith, R.B., Bruhn, R.L., 1984. Intraplate extensional tectonics of the eastern Basin-Range: inferences on structural style from seismic reflection data, regional tectonics, and thermal-mechanical models of brittle–ductile deformation. Journal of Geophysical Research 89, 5733–5762.

Standlee, L.A., 1982. Structure and stratigraphy of Jurassic rocks in central Utah: their influence on tectonic development of the Cordilleran foreland thrust belt. In: Powers, R.B. (Ed.), Geologic Studies of the Cordilleran Foreland Thrust Belt. Rocky Mountain Association of Geologists, pp. 357–382.

Suppe, J., Medwedeff, D.W., 1990. Geometry and kinematics of fault propagation folding. American Association of Petroleum Geologist Bulletin 83, 409–454.

Sussman, A.J., 1995. Geometry, deformation history and kinematics in the footwall of the Canyon Range thrust, central Utah. M.S. thesis, University of Rochester, Rochester, New York, 120pp.

Thomas, W.A., 1990. Controls on location of transverse zones in thrust belts. Eclogae Geologicae Helvetiae 83, 727–744.

Tooker, E.W., 1983. Variations in structural style and correlation of thrust plates in Sevier foreland thrust belt, Great Salt Lake area, Utah. In: Miller, D.M., Todd, R., Howard, K.A. (Eds.), Tectonic and Stratigraphic Studies in the Eastern Great Basin. Geological Society of America Memoir 157, pp. 61–74.

Villien, A., Kligfield, R.M., 1986. Thrusting and synorogenic sedimentation in central Utah. In: Peterson, J.A. (Ed.), Paleotectonics and Sedimentation in the Rocky Mountain Region, United States. American Association of Petroleum Geology Memoir 41, pp. 281–308.

Wang, Y.F., 1970. Geological and geophysical studies of the Gilson Mountains and vicinity, Juab County, Utah. Ph.D. dissertation, University of Utah, Salt Lake City, 196pp.

Wojtal, S.F., 1982. Finite deformation in thrust sheets and their material properties. Ph.D. dissertation, Johns Hopkins University, Baltimore, Maryland, 313pp.

Wood, D.S., 1973. Patterns and magnitudes of natural strain in rocks. Philosophical Transactions Royal Society of London A274, 373–382.